

2 cop.

3416
MASTER

RECEIVED BY DITE APR 1 1971

Contract Report

SC-CR-69-3277
January 1971

**ELECTROSTATIC METHODS TO CONTROL PLACEMENT
AND ORIENTATION OF SHORT GRAPHITE FIBERS
Final Report**

R. B. Reif
L. R. Albrechtson
J. H. Walder
M. C. Brockway
F. P. Kirkhart
L. E. Walkup
Battelle Memorial Institute
For:
Sandia Laboratories, Albuquerque

SANDIA LABORATORIES



OPERATED FOR THE UNITED STATES ATOMIC ENERGY COMMISSION BY SANDIA CORPORATION | ALBUQUERQUE, NEW MEXICO. LIVERMORE, CALIFORNIA

DISTRIBUTION OF THIS DOCUMENT IS UNLIMITED

DISCLAIMER

This report was prepared as an account of work sponsored by an agency of the United States Government. Neither the United States Government nor any agency Thereof, nor any of their employees, makes any warranty, express or implied, or assumes any legal liability or responsibility for the accuracy, completeness, or usefulness of any information, apparatus, product, or process disclosed, or represents that its use would not infringe privately owned rights. Reference herein to any specific commercial product, process, or service by trade name, trademark, manufacturer, or otherwise does not necessarily constitute or imply its endorsement, recommendation, or favoring by the United States Government or any agency thereof. The views and opinions of authors expressed herein do not necessarily state or reflect those of the United States Government or any agency thereof.

DISCLAIMER

Portions of this document may be illegible in electronic image products. Images are produced from the best available original document.

Issued by Sandia Corporation
a prime contractor to the
United States Atomic Energy Commission

NOTICE

This report was prepared as an account of work sponsored by the United States Government. Neither the United States nor the United States Atomic Energy Commission, nor any of their employees, nor any of their contractors, subcontractors, or their employees, makes any warranty, express or implied, or assumes any legal liability or responsibility for the accuracy, completeness or usefulness of any information, apparatus, product or process disclosed, or represents that its use would not infringe privately owned rights.

SC-CR-69-3277

ELECTROSTATIC METHODS TO CONTROL PLACEMENT
AND ORIENTATION OF SHORT GRAPHITE FIBERS

Final Report

Prepared by

R. B. Reif, L. R. Albrechtson,
J. H. Walder, M. C. Brockway,
F. P. Kirkhart, and L. E. Walkup
Battelle Memorial Institute
Columbus Laboratories
Columbus, Ohio 43201

for

Sandia Laboratories
Albuquerque, New Mexico 87115
Irving Auerbach - Consultant

Sandia Order No. FAO 48-7896

January 1971

LEGAL NOTICE

This report was prepared as an account of work sponsored by the United States Government. Neither the United States nor the United States Atomic Energy Commission, nor any of their employees, nor any of their contractors, subcontractors, or their employees, makes any warranty, express or implied, or assumes any legal liability or responsibility for the accuracy, completeness or usefulness of any information, apparatus, product or process disclosed, or represents that its use would not infringe privately owned rights.

DISTRIBUTION OF THIS DOCUMENT IS UNLIMITED

TABLE OF CONTENTS

	<u>Page</u>
INTRODUCTION	7
SUMMARY.	8
CONCLUSIONS AND RECOMMENDATIONS.	9
EXPERIMENTAL WORK AND DISCUSSION	11
Raw Materials Characterization	11
Fiber Size Distribution	11
Crystallographic Characteristics and Density.	12
Classification of Fibers	14
Roll-Type Classifier	14
Nonuniform Field Classifier.	15
D.C. Operation.	17
A.C. Operations	19
Fiber Orientation Studies.	22
Induction Systems	22
Field Alignment	24
Corona Deposition	25
Preparation of Samples	26
Bench-Model Coater.	27
Substrate Studies	28
Graphite Fibers	29
Composites.	29
Rayon Fibers.	33
Reciprocating Bench-Model Coater.	34
Graphite Fibers	35
Composites.	37
Characterization of Deposits.	37
Processing of Deposits	43
Infiltration.	43
Uniaxial Pressing	44
Isostatic Pressing.	44

LIST OF TABLES

TABLE 1. RELATION OF FIBER DEPOSITION TO SUBSTRATE ON BENCH-MODEL COATER.	28
TABLE 2. COMPOSITES PREPARED ON BENCH-MODEL COATER.	30
TABLE 3. COMPOSITES PREPARED ON RECIPROCATING COATER.	38

LIST OF FIGURES

	<u>Page</u>
FIGURE 1. MICROPHOTO OF AS-RECEIVED D9 14 01 CARBON FIBERS.	11
FIGURE 2. FREQUENCY DISTRIBUTION OF L/D MEASURED ON A 200 FIBER SAMPLE FROM AS-RECEIVED FIBER LOT D9 14 01.	13
FIGURE 3. ROLL TYPE CLASSIFIER.	14
FIGURE 4. MOVEMENT OF CHARGED FIBER IN NONUNIFORM ELECTRICAL FIELD.	16
FIGURE 5. NONUNIFORM FIELD SEPARATOR.	18
FIGURE 6. SMALL SIZE "WHISKER" FRACTION OF ELECTROSTATIC SEPARATION OF D9 14 01 FIBERS IN A NONUNIFORM ELECTRIC FIELD	20
FIGURE 7. INTERMEDIATE PRODUCT FROM ELECTROSTATIC SEPARATION OF D9 14 01 FIBERS IN A NONUNIFORM ELECTRIC FIELD.	21
FIGURE 8. LARGE SIZE FRACTION OF ELECTROSTATIC SEPARATION OF D9 14 01 FIBERS IN A NONUNIFORM ELECTRIC FIELD.	21
FIGURE 9. ELECTROCOATING.	22
FIGURE 10. INDUCTION CHARGING AND CORONA DEPOSITION.	23
FIGURE 11. INDUCTION CHARGING WITH FIELD DEPOSITION.	23
FIGURE 12. POLARIZATION ALIGNMENT.	24
FIGURE 13. CORONA DEPOSITION METHOD.	26
FIGURE 14. BENCH-MODEL COATER.	27
FIGURE 15. D9 14 01 FIBER DEPOSIT VIEWED APPROXI- MATELY PERPENDICULAR TO THE DEPOSIT SURFACE	31
FIGURE 16. FIBER AND THERMAX (5 w/o) POWDER VIEWED APPROXIMATELY PERPENDICULAR TO THE DEPOSIT SURFACE	31
FIGURE 17. FIBER AND THERMAX (15 w/o) POWDER VIEWED APPROXIMATELY PERPENDICULAR TO THE DEPOSIT SURFACE	31
FIGURE 18. FIBER AND THERMAX (25 w/o) POWDER VIEWED APPROXIMATELY PERPENDICULAR TO THE DEPOSIT SURFACE	31

LIST OF FIGURES (Continued)

	<u>Page</u>
FIGURE 19. FIBER AND THERMAX (25 w/o) POWDER VIEWED APPROXIMATELY PERPENDICULAR TO THE DEPOSIT SURFACE .	32
FIGURE 20. FIBER AND 988 C GRAPHITE (5 w/o) POWDER VIEWED APPROXIMATELY PERPENDICULAR TO THE DEPOSIT SURFACE .	32
FIGURE 21. FIBER AND 988 C GRAPHITE (15 w/o) POWDER VIEWED APPROXIMATELY PERPENDICULAR TO THE DEPOSIT SURFACE.	32
FIGURE 22. FIBER AND 1264 GRAPHITE (5 w/o) POWDER VIEWED APPROXIMATELY PERPENDICULAR TO THE DEPOSIT SURFACE.	32
FIGURE 23. FIBER AND 18666-88 GRAPHITE (5 w/o) POWDER VIEWED APPROXIMATELY PERPENDICULAR TO THE DEPOSIT SURFACE.	33
FIGURE 24. RECIPROCATING COATER	34
FIGURE 25. ELECTROSTATICALLY DEPOSITED CARBON FIBERS PLUS COAL TAR PITCH AND SOLVENT	35
FIGURE 26. ELECTROSTATICALLY DEPOSITED CARBON FIBERS PLUS MICRONIZED COAL TAR PITCH.	36
FIGURE 27. ELECTROSTATICALLY DEPOSITED CARBON FIBERS PLUS MICRONIZED COAL TAR PITCH.	36
FIGURE 28. POLISHED SECTIONS OF 5AG/F AFTER IMPREGNATION WITH EPOXY .	39
FIGURE 29. POLISHED SECTIONS OF 5SP/F AFTER IMPREGNATION WITH EPOXY .	40
FIGURE 30. POLISHED SECTIONS OF 10 MP/F AFTER IMPREGNATION WITH EPOXY	41
FIGURE 31. POLISHED SECTIONS OF 10 P/F AFTER IMPREGNATION WITH EPOXY	42
FIGURE 32. UNIAXIALLY PRESSED 10 MP/F VIEWED PERPENDICULAR TO THE DIRECTION OF PRESSURE	45
FIGURE 33. POLISHED SECTIONS OF 10 MP/F UNAXIALLY WARM PRESSED AND BAKED, THEN IMPREGNATED WITH EPOXY	46
FIGURE 34. ISOSTATICALLY PRESSED 5AG/F	47

ELECTROSTATIC METHODS TO CONTROL PLACEMENT AND
ORIENTATION OF SHORT GRAPHITE FIBERS

FINAL REPORT

INTRODUCTION

Nose cones are subjected to severe environmental conditions such as high temperatures, severe thermal shock, oxidizing atmosphere, and mechanical stresses during reentry. Bulk graphites have shown considerable potential as construction materials for nose cones of reentry vehicles. Since mass loss during reentry (ablation) is a combination of oxidation, mechanical wear, and thermal spallation, various grades of bulk graphites have been developed which exhibit properties that cause them to resist one or another of the environmental conditions. Thus some grades resist ablation better than others. Recent work at the Union Carbide Y-12 Plant at Oak Ridge, Tennessee has provided a grade of bulk/composite graphite that in limited testing appears to resist ablation better than most graphites. This material is composed of short carbon/graphite fibers in a coal tar pitch matrix. Fibers being used are reportedly about 2 μ diameter by about 10 mils long. They are carbonized as short fibers from a cellulose base (rayon) precursor. Molding and impregnation operations are used to fabricate bulk materials from the fibers and liquid pitch.

One problem in forming a homogeneous material from short fibers involves the prevention of fiber agglomerations. The fibers have a high affinity for each other because of the large surface area and large electrostatic surface charge. Another problem is that of controlled orientation of the fibers in the bulk material. The method commonly used to deagglomerate fibers is to screen them and allow them to free-fall into the molding container. This results in two dimensional orientation of the fibers.

The common method used to randomize the fibers in the above bulk material is to break up the material at an early stage in the process cycle into small, more-or-less equiaxial particles and then mold the particles together with additional pitch.

The purpose of this program was to study electrostatic methods to control both the placement and orientation of short carbon/graphite fibers and carbon base particulate fiber material in a bulk graphite matrix and to characterize resulting experimental structures.

SUMMARY

Several electrostatic methods were evaluated for classifying graphite fibers according to size and length. Both static and alternating fields were used in roll-type and plate-type nonuniform field devices. The latter type showed the most promise. Dedusting or removal of fiber whiskers produced during carbonization of the fibers was accomplished with both static and alternating fields between nonparallel plates. Separation of fiber fragments, 10-mil fibers, and oversize fibers was demonstrated in the alternating field device. Further refinement of this technique should yield clean fractions of 10-mil fibers.

A number of electrostatic techniques were examined for producing oriented and isotropic structures with graphite fibers and fiber-particulate composites. The fibers were charged by induction or ion bombardment and then deposited in either an oriented or unoriented manner in an electrical field. Although orientation was obtained by certain procedures, most work was done with essentially isotropic structures. The fibers were dispersed in an air stream, charged by ion bombardment, and deposited on a substrate with an electrical field. Because the conductive fibers reversed charge inductively when deposited on a metallic surface, heavy deposits could not be made unless an adhesive or an insulating substrate such as tympan paper was used to collect the material.

The same technique was used successfully to prepare fiber composites with feed compositions of 5, 10, 15, and 25 percent Thermax carbon and other carbon particles. Addition of the carbon particles improved the deposition rate and density of the fiber structures.

Although the insulating uncarbonized rayon fiber could be deposited directly on a metal substrate, the charge retained on the fiber produced a low density structure.

The initial samples were prepared on a rotating drum-type collector surface, but the curved surface was not satisfactory for forming fiber structures thicker than about 1/8 inch. Subsequently, structures up to 1 inch thick were deposited on a similar unit with a reciprocating flat plate collector. Simultaneous deposition of a sprayed solution of coal tar or an admixture of finely pulverized coal tar accelerated the rate of deposition and increased the strength and density of the fiber structure.

The density of short fiber composite structures as fabricated was about 0.1 gm/cc. This density could be increased to about 0.5 gm/cc by infiltration with a pitch/benzene solution and uniaxially pressing at a pressure of 1 Tsi. Examination of the structures before further processing revealed a relatively random orientation of short fibers. Attempts to use the QTM analyzer to provide quantitative interpretation of the degree of orientation of fibers in any structure failed to produce the desired results. However, stereo pair photographs of electron scanning microscope images gave a good relative assessment of the ordering of fibers.

Hydrostatic and uniaxial pressing fabrication techniques were tried with thick composites. Hydrostatic pressing appears to leave the fibers somewhat broken, but relatively unoriented in the pressed structure. Uniaxial pressing appears to orient fibers with their axis perpendicular to the pressing direction.

Sink-Float separation techniques indicated that only a part of particulate carbon admixed with short fibers before electrostatic deposition was actually deposited with the fibers. However, the efficiency of deposition was increased by addition of the particles to fibers before deposition.

CONCLUSIONS AND RECOMMENDATIONS

Careful consideration of the processing and characterization results in this study leads to the following series of conclusions:

- (1) Electrostatic techniques have demonstrated the feasibility of preparing thick structures of relatively unoriented (randomly oriented short carbon/graphite fibers.

- (2) An electric field technique for controlled orientation of short carbon/graphite fibers is feasible but needs further development for application to thick structures.
- (3) Electrostatic techniques for simultaneous placement of short fibers and carbon base particulate materials in thick bulk structures are feasible.
- (4) Particulate carbon additives or pitch (either in particulate or solution sprayed form) increase the deposition efficiency of the electrostatic techniques.
- (5) Isostatic processing applied directly to electrostatically randomized short fiber structures is feasible.
- (6) Uniaxial pressing may be used for two dimensional orientation of short fibers in a composite structure.
- (7) No convenient method for quantitatively determining the orientation of fibers in short fiber structures is available.

This program has demonstrated the feasibility of using electrostatic techniques to randomize the orientation of fibers in short fiber graphite composite structures. Processing studies have led to the conclusion that isostatic pressing may be used directly on these structures to fabricate and densify them. Ablation tests at Sandia have shown the need for a homogeneous, short fiber graphite material. These considerations have led to the following recommendations regarding short fiber materials:

- (1) Provide for the design and construction of electrostatic equipment suitable for producing useful size structures for end application (full scale testing).
- (2) Prepare useful size structures of short fibers with micronized pitch or pitch/solvent spray.
- (3) Process part of the structures of (2) using hot isostatic techniques with pitch infiltration or impregnation.
- (4) Provide structures similar to those used in (3) for processing at Oak Ridge National Laboratory.
- (5) Determine characteristic properties of materials processed in (3) and (4).
- (6) Provide ablation test models for Sandia testing.
- (7) Further develop feasible techniques for two-dimensional orientation of short fibers in structures of useful size.

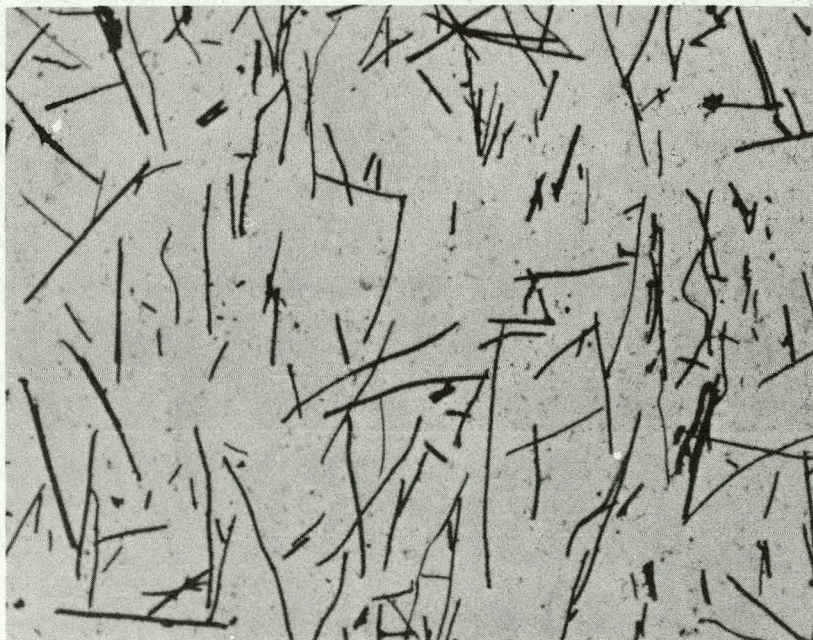
EXPERIMENTAL WORK AND DISCUSSION

Raw Materials Characterization

Raw material short carbon fibers were supplied by Sandia. They were given only minor characterization examination to determine their size, shape, density, and crystallographic character.

Fiber Size Distribution

The fibers used in this study were primarily from a lot designated as D9-14-01. It was expected that these fibers were nominally 2 microns in diameter and 10 mils long. However, Figure 1 clearly illustrates that there was a rather wide spread in diameter as well as the length of these as-received fibers. Also there was a small "whisker-like" size fraction which is shown as small "background particles" in Figure 1. This small fraction is shown more clearly in the electron scanning microscope photo (Figure 6).



100X

FIGURE 1. MICROPHOTO OF AS-RECEIVED
D9 14 01 CARBON FIBERS

In order to obtain an approximate measure of the size distribution of the primary chopped fibers, a sample of the as-received fibers was sprinkled onto a glass microscope slide and a visual size determination was then made for 200 of the fibers displayed on the slide. For this sample the fiber diameters ranged from a low of 3 microns to a high of 8 microns, with most in the 4 to 5 micron range. The lengths ranged from 90 to 270 microns. Thus, there is a rather broad distribution in the L/D ratio of these fibers. This is illustrated by the bar graph of Figure 2.

Crystallographic Characteristics and Density

The crystallographic interlayer, "d", spacing of carbon short fibers was determined by X-ray diffraction. Three samples were prepared using about 80 w/o fibers and 20 w/o NaCl powder. Using copper K α radiation, the samples were scanned in a diffractometer from about 53°2 θ to about 58°2 θ . The 222 diffraction peak of NaCl is used as a standard in this examination. It falls at precisely 56.5200°2 θ at 25°C. The difference between this angle and the observed position of NaCl in the scan is used to correct the observed 004 carbon peak. The corrected position then is used with Bragg's law to calculate the interlayer spacing of carbon. This calculation for the three fiber samples gave interlayer spacings of 3.4033, 3.4010, and 3.3988 Å. These interlayer spacings are indicative of highly turbostratic material.

The density of fibers was determined by benzene displacement and by sink-float techniques. The benzene displacement technique yielded an average density of 1.42 gm/cc. The sink-float technique using benzene in carbon tetrachloride indicated a gradation of density ranging from about 1.4 to 1.5 gm/cc.

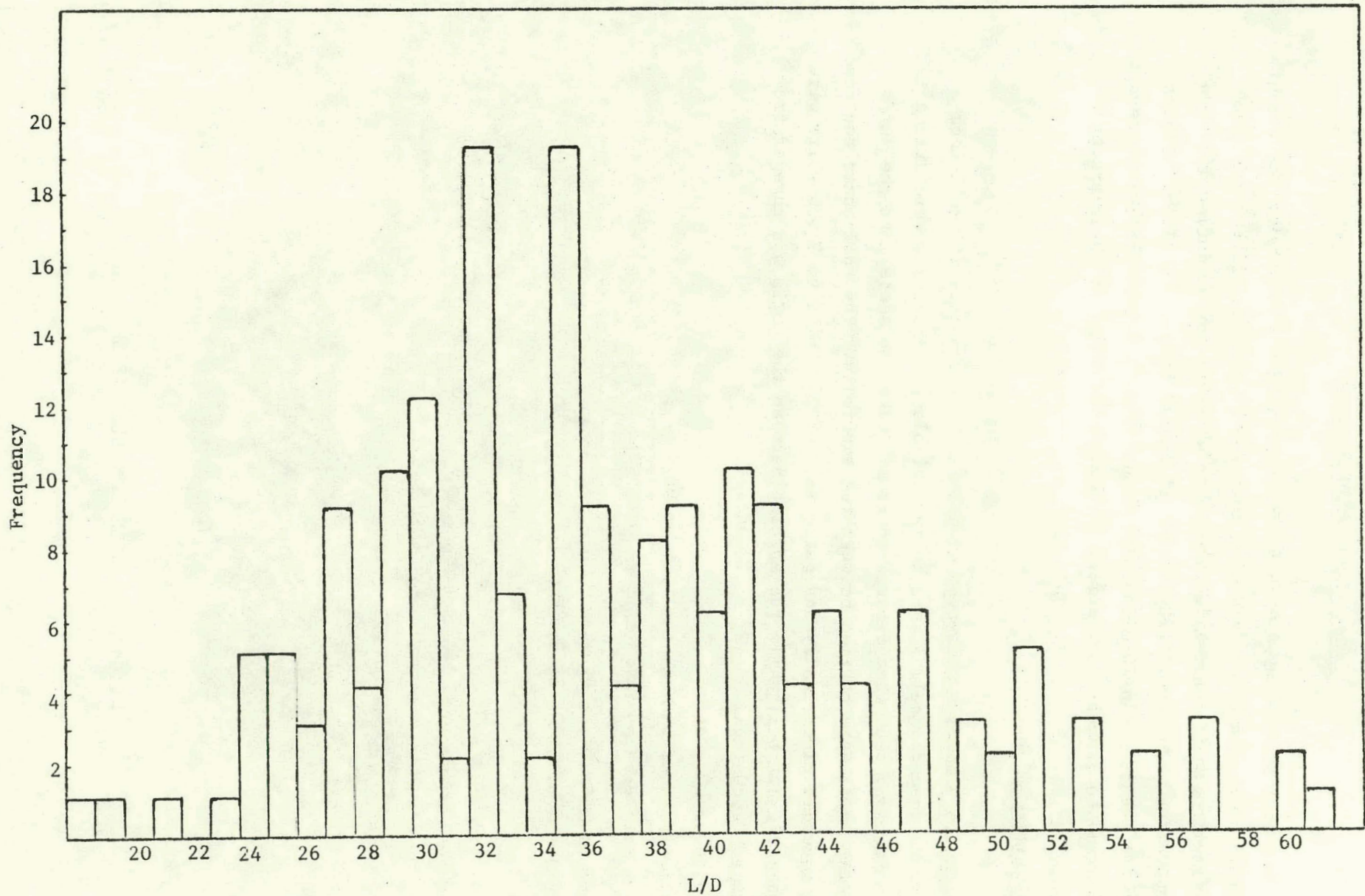


FIGURE 2. FREQUENCY DISTRIBUTION OF L/D MEASURED ON A 200 FIBER SAMPLE FROM AS-RECEIVED FIBER LOT D9 14 01.

Classification of Fibers

Electrostatic techniques were investigated for classifying the graphitized fibers. Initial studies indicated that the graphitized fibers contained four size fractions: (1) dust-like fine fiber whiskers formed during the carbonizing operation, (2) 10-mil fibers, (3) fractured bits of the 10-mil fibers, and (4) fibers greater than 10 mils long. Nonuniform field and roll-type separators were examined as means for effecting size separations of these fractions.

Roll-Type Classifier

Figure 3 shows a roll-type classifier. It consists of two 2-inch diameter rolls spaced parallel in a horizontal plane. The rolls were driven in opposite directions such that fibers fed from a vibrated chute onto the surface of one of the rolls were carried between the two rolls. The roll under the feed chute was grounded electrically and potentials of 150 volts to 3,000 volts were applied on the other roll while the spacing between the rolls was changed from 0.010 inch to 0.060 inch.

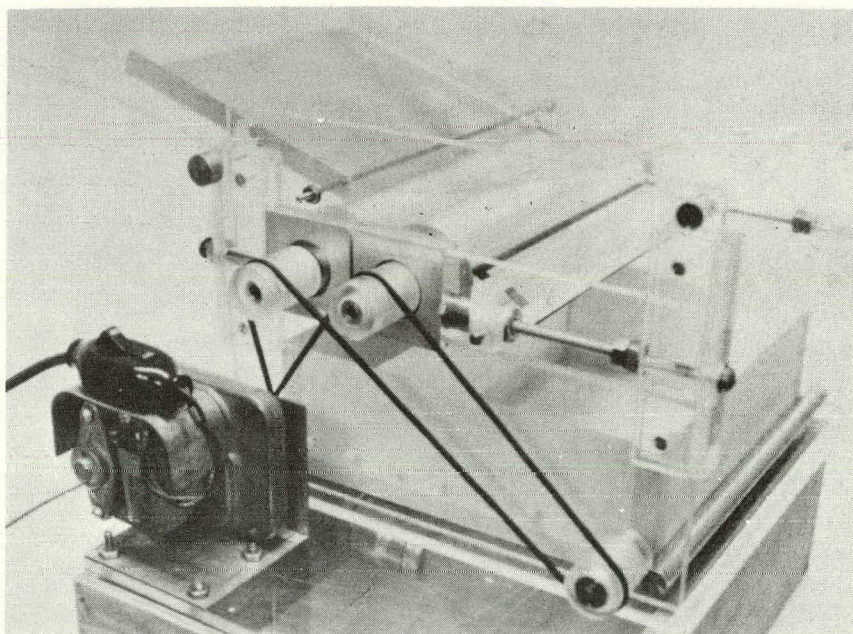


FIGURE 3. ROLL TYPE CLASSIFIER

The theory of the two roll separator is that the field in the gap between the rolls will cause the fibers to orient perpendicularly to the surface of the rolls. When the fibers enter the gap between the rolls the effective length of the gap is decreased. Long fibers decrease the gap more than the short fibers, and as a result, stronger fields exist between the long fibers and the second roll than between the short fibers and the second roll. Thus, by adjusting the gap and applied voltage so that the field is just strong enough to transfer the long fibers to the second roll, fibers of various lengths should be separated, the short fibers on one roll and the long fibers on the other.

However, with static fields applied by a d.c. power supply, fibers transferred back and forth between the rolls, but no separation of the fibers was attained. The fibers usually formed chains that shorted out the electrodes in gaps smaller than 0.025 inch, or jumped to the high voltage roll where the polarity of the charge reversed by induction and returned to the ground roll where the process repeated. Covering the high voltage roll with 0.005-inch Mylar stopped the fibers from reversing charge and returning to the ground roll but failed to effect classification of the fibers. In general increasing the voltage increased the amount of fibers transferred until all of the fibers transferred.

Some classification of the fibers was obtained with an alternating potential between the rolls while the rolls were stationary. With 60-Hz potentials of 400 to 700 volts on the high voltage roll, all of the 10-mil fibers transferred in a line at the nip between the rolls. The fiber fragments migrated to separate zones on either side of the nip. Rotating the rolls destroyed the separation effect, however.

Nonuniform Field Classifier

The basic nonuniform-field separator consists of two nonparallel plates with one of the plates grounded and the other plate at a high electrical potential. The electrical field intensity, E , at any point between the plates is determined by the ratio of the applied voltage difference, V , to the spacing, S , between the plates at the point, or $E = V/S$. Inasmuch as the applied voltage difference is constant everywhere between the electrodes, the electrical field strength decreases as the spacing between the electrodes increases.

Figure 4 is a schematic diagram of the nonuniform-field separator showing the plate electrodes, the electrical field lines, and the path of fibers in the separator. The electrical field lines are segments of circles with centers at the intersection of the projections of the plates. A conductive fiber, placed in the field, is charged by induction while in contact with either electrode. When the charge is sufficient, the force exerted by the electrical field carries the fiber to the other electrode where the process is repeated. As the fiber bounces back and forth, it migrates into the lower field area. The same effect can be attained with insulating fibers by precharging the fibers and then alternating the direction of the electrical field.

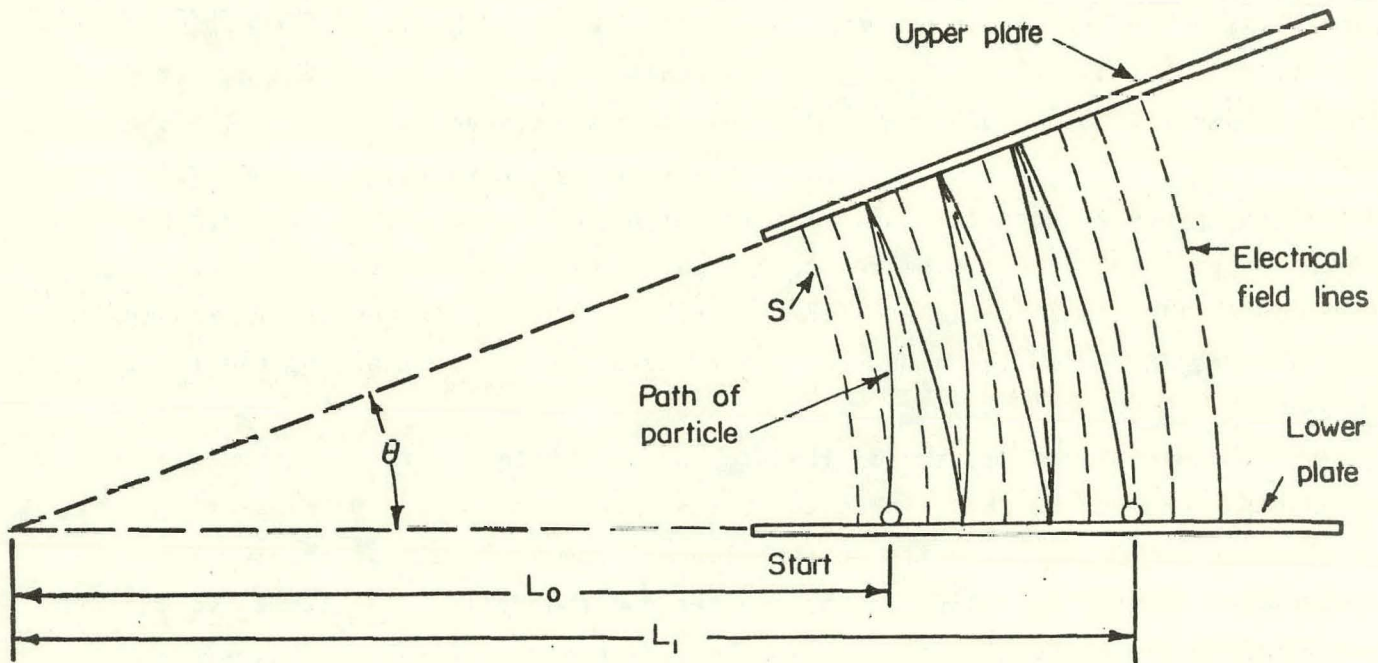


FIGURE 4. MOVEMENT OF CHARGED FIBER IN NONUNIFORM ELECTRICAL FIELD

The movement of fibers toward the low-field areas (to the right in Figure 4) is caused by centrifugal force acting on fibers being accelerated along the curved paths of the electrical field. The centrifugal force is a function of the mass or length of a uniform fiber, and increases with the square of the velocity of the fiber. Inasmuch as small fibers may attain velocities of several hundred inches per second in electrical fields, centrifugal forces are effective in causing fibers to move into lower field areas of the classifier.

The final position in the separator is reached when the electrical field force is no longer sufficient to overcome the gravity force on the fiber. Since the electrical field force is a function of the charge on the surface of the fiber and the gravity force is a function of the mass of the fiber, the electrical force will decrease more slowly than the gravity force and small fibers might be expected to move farther than large fibers into the weaker electrical field region of the classifier. However, the opposite effect is obtained because the length of the fiber decreases the gap between the plate electrodes and the stronger field occurs with the longest fibers.

For the extremely small fibers with masses less than an equivalent sphere with a diameter of 40 microns, the molecular or Van der Waals force that tends to hold surfaces together is a significant factor. Electrical forces that can be applied on the extremely small fibers often are not sufficient to pull the fibers from the surface of plates or electrodes, and the fibers remain attached to the plates where originally deposited.

Figure 5 shows one form of the nonuniform field classifier which was used for making separations of fiber fractions. The classifier consists of two nonparallel flat metal electrodes which are 46 inches from side to side and 30 inches from front to back. The upper electrode is skewed at an angle to the lower horizontal electrode and is insulated from the lower electrode. A high potential is applied to the upper electrode while the lower electrode is grounded.

D. C. Operation. Complete removal of whisker-type fragments was accomplished with the nonuniform field separator with static fields. With a minimum gap of 1 inch and a plate angle of 5 degrees, the original fiber mixture was spread in a line about 1 inch from and parallel to the edge of the high field side of the lower electrode. Voltages of 10 to 30 kv were applied on the upper electrode until movement of the fibers stopped. When 20 kv was applied, most of the 10-mil fibers moved 9 to 22 inches into the weaker field region.

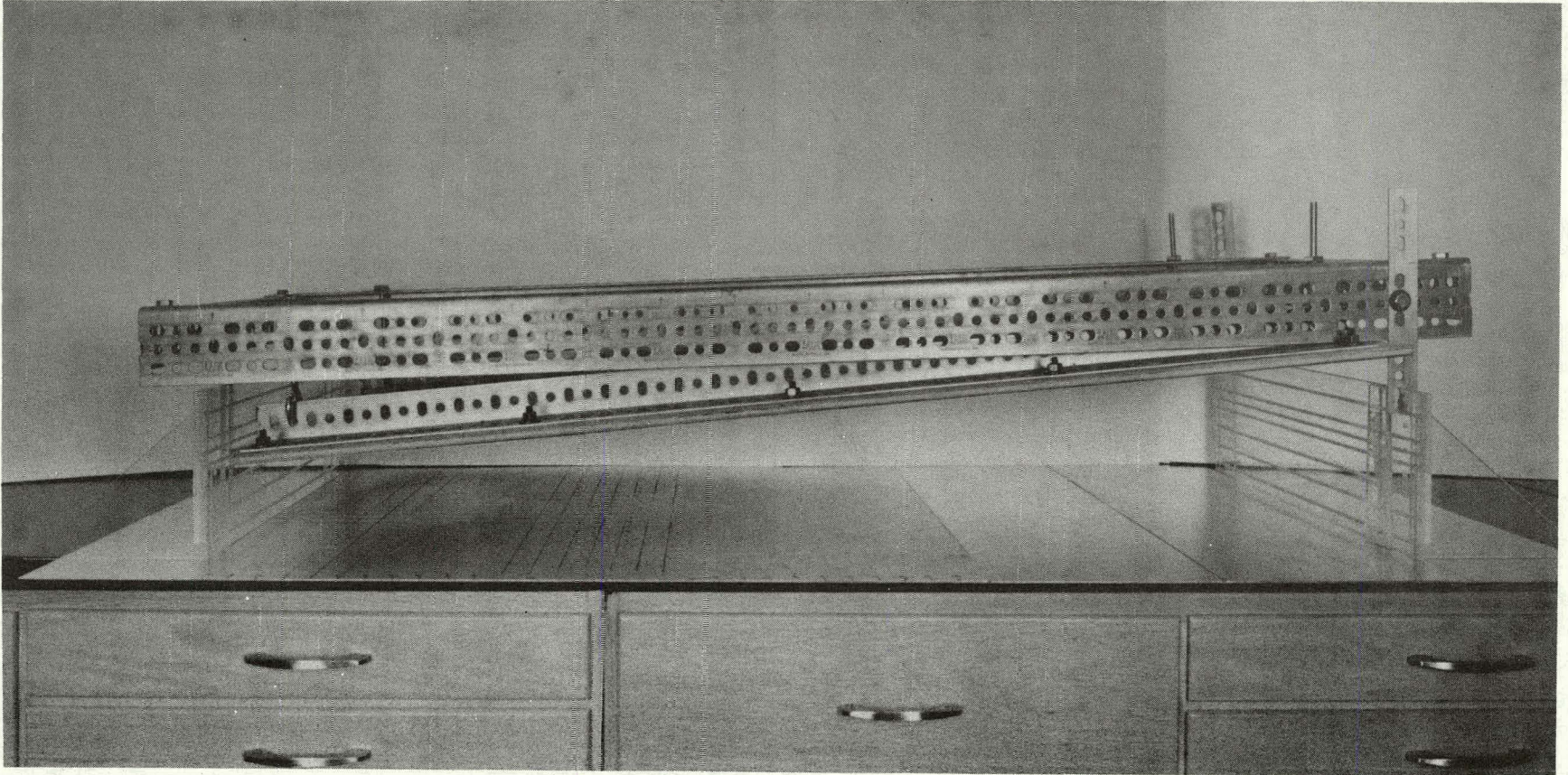


FIGURE 5. NONUNIFORM-FIELD SEPARATOR

Most of the fiber whiskers such as shown in Figure 6, some fiber fragments and a few whole fibers, remained in the first 9 inches of the separator. (See Figure 7.) The concentration of the 10-mil fibers was highest in the region from 9 to 22 inches from the high field side of the electrodes (see Figure 8). Lower voltages (10 to 15 kv) produced less movement of the fibers into the field and did not separate the fiber fractions cleanly. At 30 kv, some fibers moved as far as 34 inches into the weak field region and the fiber whiskers and fragments spread to 10 inches. The fibers in the region from 18 to 19 inches were all 10 mils long, but the 10-mil fibers were found in quantity also in the region from 10 to 28 inches. A few fibers longer than 10 mils were found in the weakest field area. Although no attempt was made to concentrate these fractions further, recycling the fractions would be expected to enhance the classification.

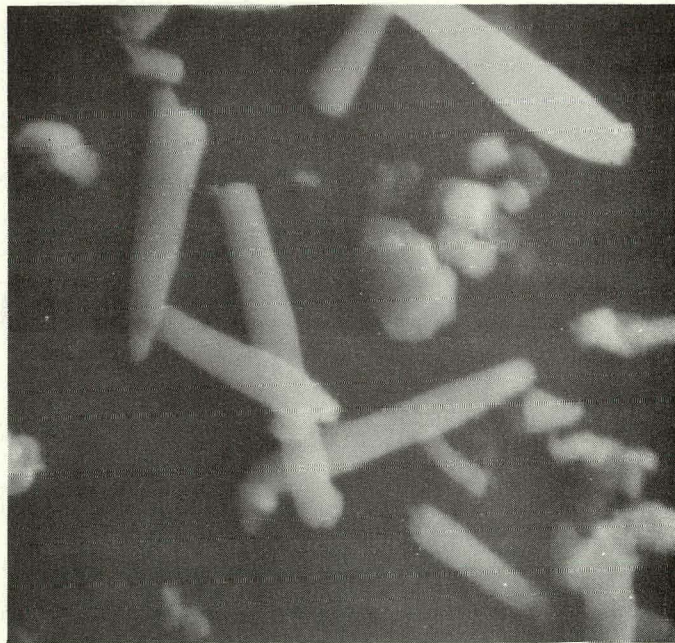
No classification of ungraphitized rayon fibers could be obtained in the nonuniform field unit when the fibers were processed in the same way as the graphite fibers.

A.C. Operations. In view of the results obtained with alternating potentials on the two-roll separator, alternating fields also were tried on the nonuniform field separator with somewhat higher angles than used with the static fields. Two 12 by 12-inch plates were spaced with a 1/2-inch gap on the high intensity field side and 1-1/2- to 4-1/2-inch gaps on the low intensity field side. Sixty-Hertz potentials of 4 to 10 kv were applied on the upper electrode while the lower horizontal electrode was grounded. As before, the fibers were placed along the edge of the lower electrode near the high field side, and the field was applied until fiber movement toward the weaker field region stopped. The best separations were obtained with 4 kv using a gap of 2-1/2 inches on the low field side. Although the fiber whiskers were not classified as with the static fields, only fiber fragments remained in the region from 0 to 3 inches from the high field side. The concentration of fragments decreased in the region between 4 and 7 inches, and beyond 8 inches the fibers were all 10 mil. The prospect of removing fiber fragments from nominal 10-mil graphite fibers in an alternating nonuniform field showed sufficient promise to merit further study.



2000X

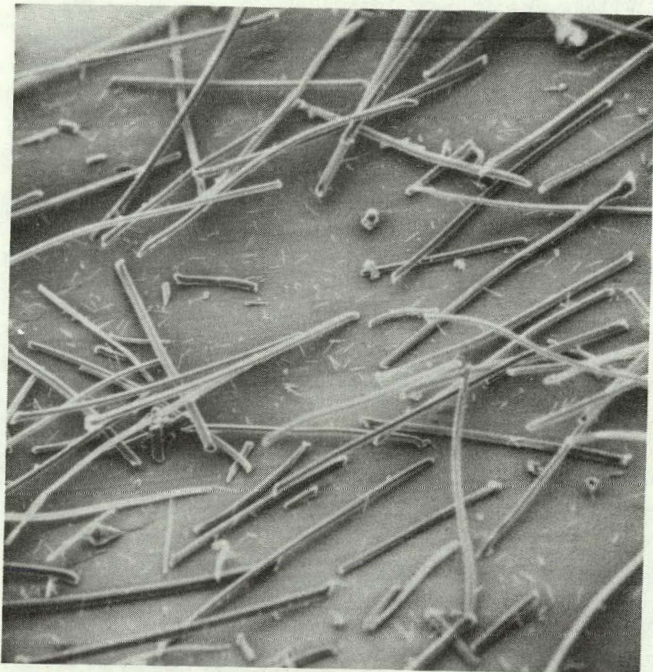
26019-6



10,000X

26019-6

FIGURE 6. SMALL SIZE "WHISKER" FRACTION OF ELECTROSTATIC SEPARATION OF D9 14 01 FIBERS IN A NON-UNIFORM ELECTRIC FIELD.

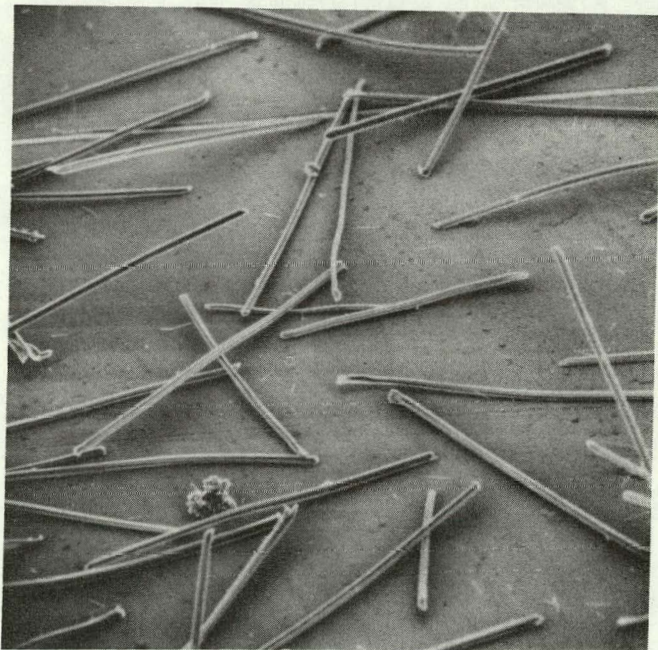


200X

26019-7

FIGURE 7.

INTERMEDIATE PRODUCT FROM
ELECTROSTATIC SEPARATION OF
D9 14 01 FIBERS IN A NON-
UNIFORM ELECTRIC FIELD.



200X

26019-8

FIGURE 8.

LARGE SIZE FRACTION OF ELECTRO-
STATIC SEPARATION OF D9 14 01
FIBERS IN A NON-UNIFORM
ELECTRIC FIELD.

Fiber Orientation Studies

A cursory examination was made of various methods for effecting orientation of the 10-mil graphite fibers. Induction charging, ion charging, and field orientation were employed. Although orientation of the fibers was demonstrated with several systems, none was developed to the degree that thick samples could be prepared with all the fibers oriented in the same direction.

Induction Systems

Orientation of the fibers parallel to the electrical field lines of force was the primary method for obtaining orientation in induction charging systems. Several variations of induction charging systems were tried.

Figure 9 shows one form of an induction charging system commonly used in electrocoating of abrasives and flocking. The apparatus consists of two parallel plate electrodes spaced 2 inches apart. Graphite fibers were placed on the lower grounded electrode as shown at A and a negative potential of 10 kv was applied on the upper electrode. The fibers acquired charge by induction from the grounded electrode in the electrical field, oriented in the field as shown at B, and then jumped to the upper electrode. Since the graphite fibers are conductive, they reversed polarity after contacting the upper electrode and bounced between the two electrodes unless the upper electrode was coated with an adhesive as at D. Multiple layers of fibers could be deposited if positively charged droplets of adhesive were sprayed along with the fibers, but this was not reduced to practice.

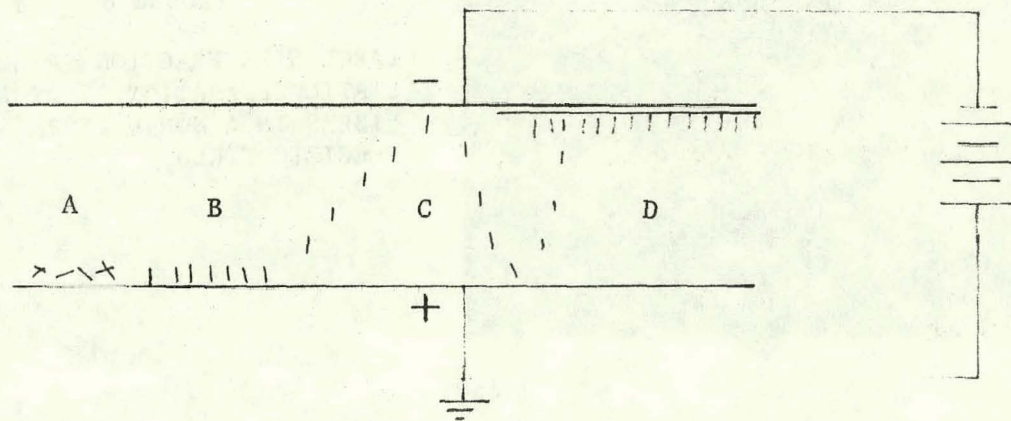


FIGURE 9. ELECTROCOATING

Other forms of induction processes are shown in Figures 10 and 11. In the system shown in Figure 10, the fibers are dropped onto a spherical electrode at a positive voltage where they are charged inductively. When the fibers receive sufficient charge to be pulled off the electrode by the electrical field, they are directed toward a negatively charged grid of 1/4-inch hardware cloth. The fibers that pass through the grid are then deposited on a rotating drum using corona from a small wire above the drum. Although the fibers were deposited on the drum, they failed to stay on the grounded drum and no significant deposit accumulated.

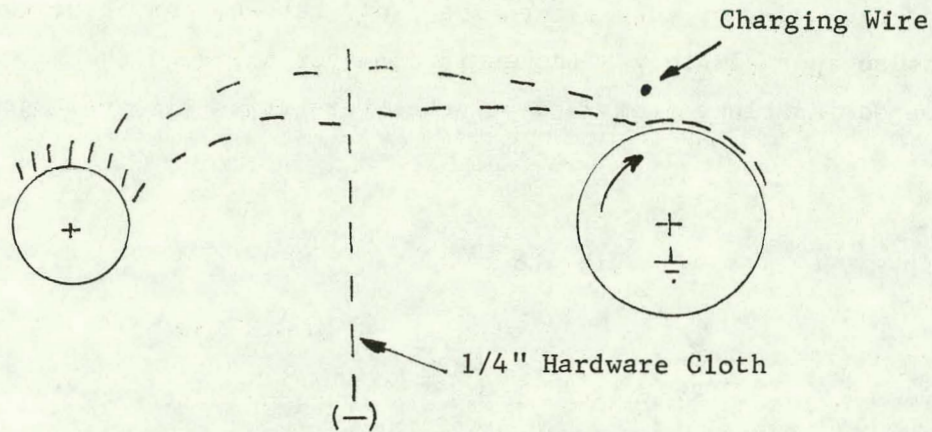


FIGURE 10. INDUCTION CHARGING AND CORONA DEPOSITION

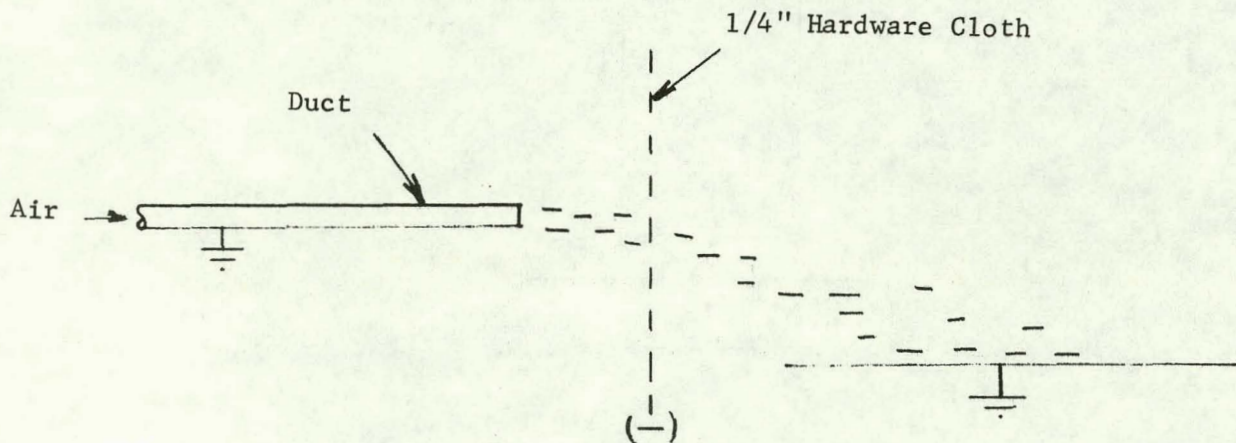


FIGURE 11. INDUCTION CHARGING WITH FIELD DEPOSITION

When the fibers were blown through a negatively charged hardware cloth grid as shown in Figure 11, they were deposited on a horizontal grounded plate. Although this technique produced orientation in long textile fibers, it failed to produce orientation with the conductive 0.010-inch graphite fibers.

Field Alignment

Alignment of fibers by polarization effects in a uniform electrical field between two parallel plates was demonstrated with the apparatus in Figure 12. The graphite fibers were screened through a 60-mesh sieve and allowed to fall through a 2-foot column into the field between the electrodes. A paperboard enclosure approximately 8 inches in diameter shielded the fibers from drafts. Electrode spacings from 2 to 4 inches were tried with voltages up to 30 kv.

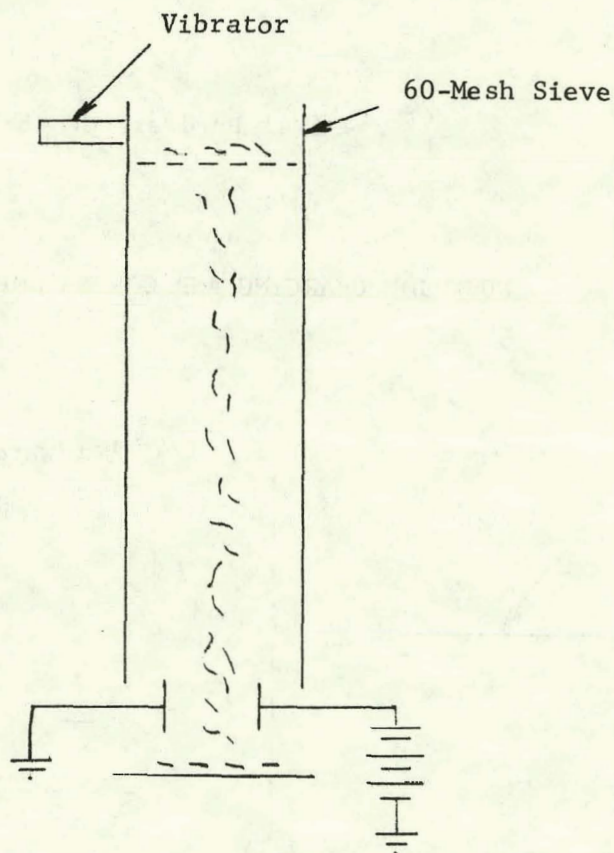


FIGURE 12. POLARIZATION ALIGNMENT

With static fields, no significant amount of alignment was obtained in the fiber collected on the horizontal plate 4 inches below the electrodes. However, the fibers collected on a sheet of paper above the electrodes were oriented parallel to the field lines between the electrodes. Maximum effect was obtained with 30 kv applied with an electrode spacing of 3 inches.

Orientation also was obtained in fibers collected on a grounded plate 2 inches below the electrodes when a 60-Hz alternating field was applied on the electrodes. In one case where the orientation was marked, 15 kv was applied across a 2-inch gap between two 6-inch-square plates while the electrodes were inclined at an angle of 30 degrees from the vertical. No attempt was made to prepare a thick deposit using these techniques because the output was very small.

Corona Deposition

Corona charging and deposition of airborne fibers was an effective method for orienting the 0.010-inch graphite fibers when the air velocity was adjusted properly. The fibers were dispersed in an air stream through a venturi inlet, delivered to the deposition zone through a slot, charged with corona, and deposited on a rotating grounded drum.

Figure 13 shows a typical arrangement of this type of apparatus. The drum used was approximately 5 inches in diameter and 10 inches wide. The two charging wires were 0.004-inch-diameter stainless steel, spaced 1-1/2-inches apart and 1 inch from the surface of the drum. Positive or negative potentials of 10 to 12 kv were applied on the wires to produce corona for charging the fibers and to produce the field for depositing the fibers on the drum. The exit slot of the delivery duct was 0.020 inches wide by 6 inches long.

At low air pressure, the orientation of the fiber deposited on the drum was poor. However, at 60 psi and higher, the fiber deposited on the drum was oriented parallel to the direction of rotation of the surface of the drum. Although the fibers were deposited at very low rates in this initial study, the system is capable of operation at much higher rates and therefore might be practical for a production process.

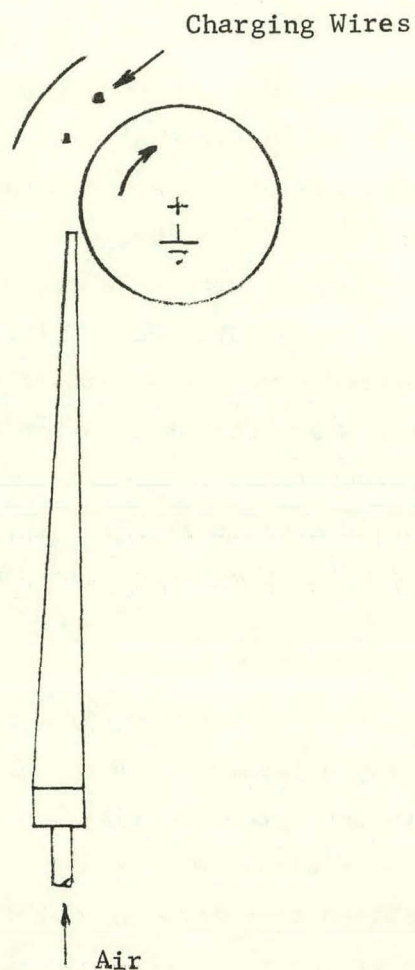


FIGURE 13. CORONA DEPOSITION METHOD

Preparation of Samples

Subsequent to the study of methods for orienting fibers, practical methods for preparing samples were considered. In this initial study, effort was concentrated on techniques that produced homogeneous structures to provide three dimensional interlocking of the fibers. Deposition of fibers from an air stream using corona to charge the fibers and to drive the fibers onto a desired site seemed the most promising method in that it has the potential of (1) providing rapid deposition rates and (2) permitting orientation of the fibers in specific modes if desired.

Bench-Model Coater

Figure 14 shows the bench-model coater that was used to prepare thin samples of graphite fibers and composites of carbon particles with graphite fibers. The unit consists of (1) an air supply and venturi to feed the fibers to the coater, (2) a duct with a 1/4-inch by 10-inch slot to distribute the fibers, (3) a pair of 0.004-inch-diameter charging wires, and (4) a rotating grounded drum on which to deposit the fibers. Air pressure from 5 to 30 psi was used to disperse and carry the fibers to the grounded drum, and a negative potential of 5 to 20 kv was applied on the wires at a distance of 1 inch to deposit the fibers on the drum. Although the rayon fibers could be deposited directly on the metal drum, the graphite fibers would not remain on the drum after they were deposited. Apparently they reversed polarity by induction in the fringe area of the electrical field and were blown off.

Preliminary studies indicated that layers of the graphite fibers could be deposited by applying an adhesive on the conductive surface or by placing a substrate sheet of 6-mil tympan paper on the metal drum.

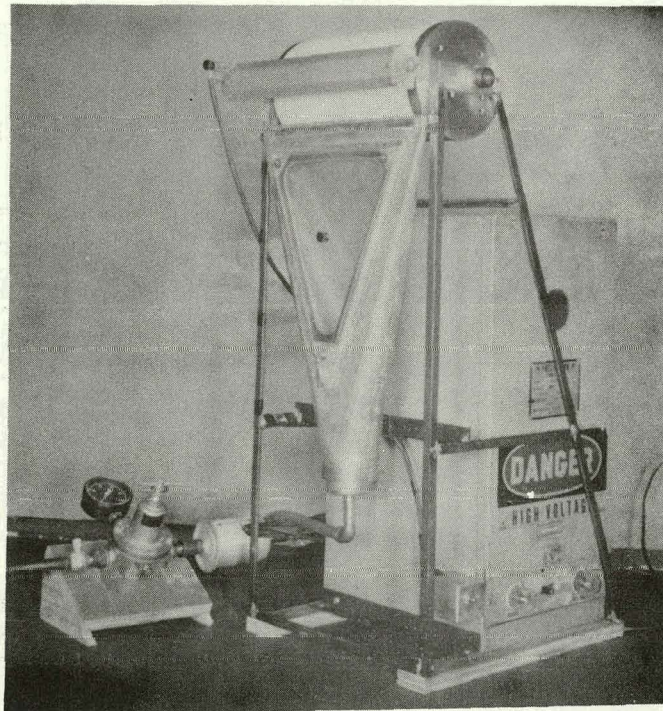


FIGURE 14. BENCH-MODEL COATER

Substrate Studies. A brief search was made to find a substrate material that would provide optimum deposition of the fibers on the bench-model coater. A 5 by 5-inch sheet of each of the materials listed in Table 1 was taped onto the drum of the coater, and 2 grams of powder was fed to the coater and deposited on the sheets. The amount of powder deposited on each sheet is given in milligrams in the table.

Resistivity of each of the materials was calculated from measurements of the current that flowed through a pair of 2-inch circular electrodes with a potential of 500 volts applied across the sample.

Data in Table 1 show that the heaviest deposition was obtained on 6-mil tympan paper. The second best substrate was 30 mils of red rubber. The deposition was unrelated to the resistivity of the substrate, however, inasmuch as the resistivity of the tympan paper was of the order of 10^9 ohm-centimeters while that of the rubber was 10^{14} ohm-centimeters. Deposition on the other materials which had resistivities of either order was only a fraction of that obtained on the two best substrates. Deposition of the fibers obviously was controlled by factors other than resistivity, but no further study was made to identify the factors.

Tympan paper was selected for the deposition substrate in these studies.

TABLE 1. RELATION OF FIBER DEPOSITION TO SUBSTRATE ON BENCH MODEL COATER

Substrate	Thickness, mils	Resistivity, (a) ohm-centimeters	Relative Fiber Deposit (b)
Teflon	5	1.0×10^{16}	39
Polyethylene	4	5.6×10^{15}	7
Tympan Paper	6.5	6.5×10^9	99
Rubber Dam	11	1.7×10^{15}	31
Mylar	5	5.8×10^{15}	5
Mylar	2	3.3×10^{15}	8
Rubber	18.5	3.3×10^{12}	8
Rubber (Fiber)	16	1.2×10^6	5
Rubber (Fiber)	25	4.5×10^{10}	19
Red Rubber	30	2.5×10^{14}	87
Polypropylene	1.5	8.0×10^{14}	29
Polyethylene	2	1.7×10^{15}	4
Polycarbonate	3	2.2×10^{15}	8

(a) Measured at 500 volts.

(b) Milligrams of fiber deposited on 5 by 5-inch sheet when 2 grams of fiber were fed into coater.

Graphite Fibers. The deposition of graphite fibers on the bench-model coater was slow even with the tympan paper substrate. With a positive potential of 10 to 12 kv on the charging wire at a distance of 1 inch from the coating drum, about 3 hours was required to deposit 1/16 inch of fiber. Part of the difficulty was caused by the need to feed the material slowly to avoid excessive blow-by.

Composites. Composite structures consisting of graphite fibers and various carbon particulate were prepared on the bench-model coater. The fibers and particulate were mixed thoroughly by tumbling before they were fed into the coater with 7 psi air and deposited with positive 10 kv on the charging wires.

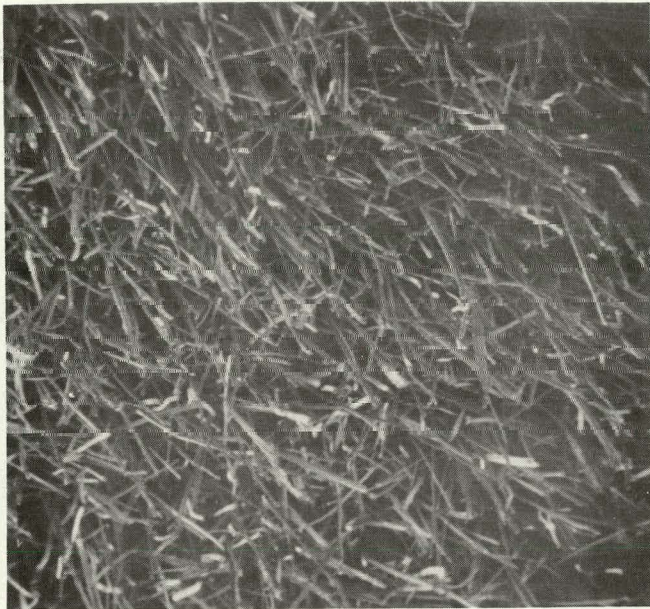
Table 2 lists the composite compositions fed to the coater plus one all-fiber example (26019-19) for comparison. The composites were deposited on tympan paper; however, those with 15 to 25 percent particulate loading could be deposited on the metal drum as well. In general, the deposition efficiency of the fiber plus particulate mixtures was better than that obtained with the graphite fibers alone; however, three hours still was necessary to produce each sample listed in Table 2. The thickness of the deposit is an indication of the deposition efficiency.

The fiber deposits listed in Table 2 were measured and weighed to obtain bulk density and were qualitatively characterized for fiber orientation by scanning electron microscopy. To estimate bulk density, the deposit thickness was measured with a binocular microscope at 30X, the area was measured, and the deposit was weighed. The data show no gross differences in as-deposited densities. The scanning electron microscopy (Figures 15-23) was conducted primarily on the surface of the plane of the deposit with a viewing angle approximately 90° to the deposit. Such viewing avoided the possibility of fiber reorientation resulting from sectioning the deposit for viewing at other angles. There is the question of whether the fibers in the top surface are oriented the same as in the interior, but it was felt this uncertainty was less serious than possible reorientation in sectioning. (In the case of thicker deposits, discussed later, sections were obtained and examined by optical microscopy.) The last column in Table 2 provides a qualitative judgement as to whether the fibers were preferentially oriented and if so, the preferred direction. The indicated orientations should not be ascribed much importance, but they do suggest that inclusion of particulate materials may alter fiber orientation perceptibly.

TABLE 2. COMPOSITES PREPARED ON BENCH-MODEL COATER

Sample Designation	Composition Fed Into Coater ⁽¹⁾ , wt. %				Deposit Thickness ⁽²⁾ inches	Approximate Deposit Density ⁽³⁾ , g/cc	ESM Microphotos ⁽⁴⁾ of Deposit	Preferred Orientation ^(4a) of Fibers
	Carbon Fiber	Type	Nominal Size	Amount				
26019-19	100	--	--	--	.045	0.16	Figure 15	Vertical
26019-21	95	Thermax	<74 microns ⁽⁵⁾	5	.069	0.17	Figure 16	Horizontal
26019-15	90	Thermax	<74 microns ⁽⁵⁾	10	.095	0.22	No Photo	--
26019-22	85	Thermax	<74 microns ⁽⁵⁾	15	.083	0.15	Figure 17	Horizontal
26019-18	75	Thermax	<74 microns ⁽⁵⁾	25	.092	0.18	Figure 18 & 19	Random
26019-24	95	988 C ⁽⁶⁾	53 to 74 microns	5	.078	0.17	Figure 20	Random
26019-25	85	988 C ⁽⁶⁾	53 to 74 microns	15	.059	0.21	Figure 21	Vertical
26019-26	95	1264 ⁽⁷⁾	74 to 105 microns	5	.075	0.17	Figure 22	Vertical
26019-23	95	18666-88 ⁽⁸⁾	2 to 30 microns	5	.035	0.18	Figure 23	Horizontal

- (1) The deposited composition is not necessarily that of the feed composition, approximate checks on the deposit compositions indicated they were lower in powder constituent than the feed composition.
- (2) Thickness was estimated by measuring with a binocular microscope at 30 X.
- (3) Density was estimated from the deposit volume (thickness x area) and weight.
- (4) All photos shown were taken at approximately 90° to the deposit surface.
- (4a) This is a very qualitative judgment of fiber orientation in reference to the plane of deposition and is based on examination of stereo pairs of the ESM photos.
- (5) Ultimate particle size of the thermax is ~0.3 microns, the agglomerates were <74 microns according to the suppliers specifications.
- (6) A natural Ceylon graphite powder.
- (7) An artificial graphite powder.
- (8) An artificial graphite powder.

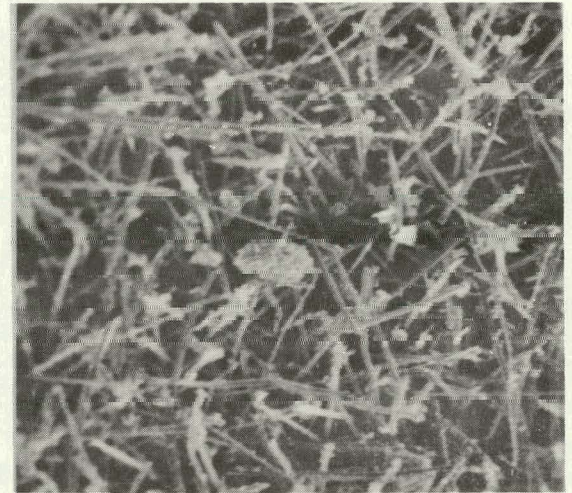


100X

26019-19-1

FIGURE 15.

D9 14 01
FIBER DEPOSIT VIEWED APPROXI-
MATELY PERPENDICULAR TO THE
DEPOSIT SURFACE



200X

26019-1

FIGURE 16.

FIBER AND
THERMAX (5 w/o) POWDER VIEWED
APPROXIMATELY PERPENDICULAR TO
THE DEPOSIT SURFACE. (A THERMAX
AGGLOMERATE IS VISIBLE IN THE CENTER
OF THE PHOTO.)

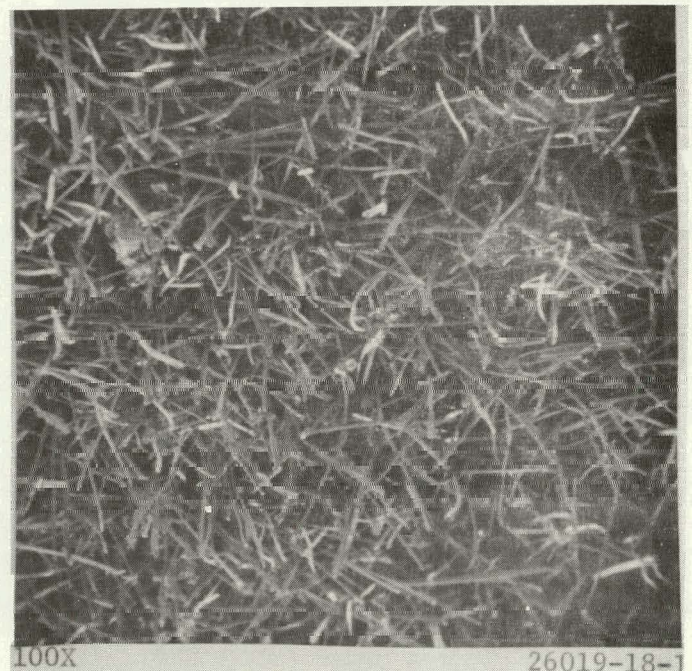


200X

26019-22

FIGURE 17.

FIBER AND
THERMAX (15 w/o) POWDER VIEWED
APPROXIMATELY PERPENDICULAR TO
THE DEPOSIT SURFACE.



100X

26019-18-1

FIGURE 18.

FIBER AND
THERMAX (25 w/o) POWDER VIEWED
APPROXIMATELY PERPENDICULAR
TO THE DEPOSIT SURFACE.

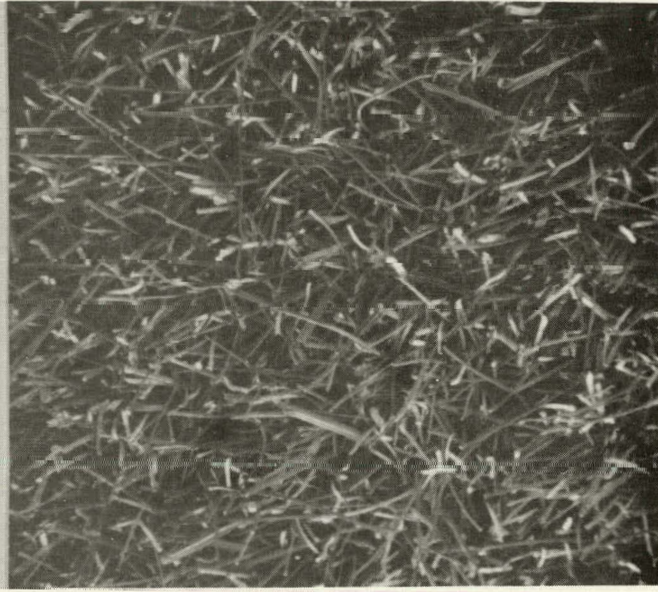


500X

26019-18-1

FIGURE 19.

FIBER AND
THERMAX (25 w/o) POWDER VIEWED
APPROXIMATELY PERPENDICULAR TO
THE DEPOSIT SURFACE.

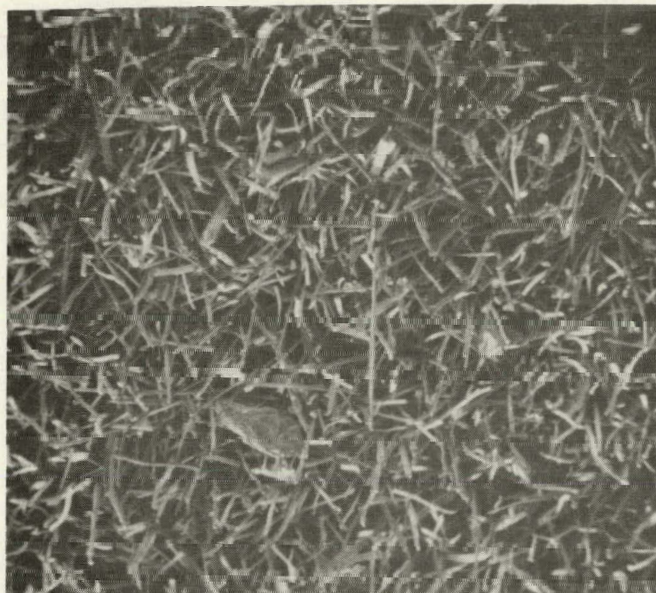


100X

26019-24

FIGURE 20.

FIBER AND
988 C GRAPHITE (5 w/o) POWDER
VIEWED APPROXIMATELY PERPENDICULAR
TO THE DEPOSIT SURFACE.

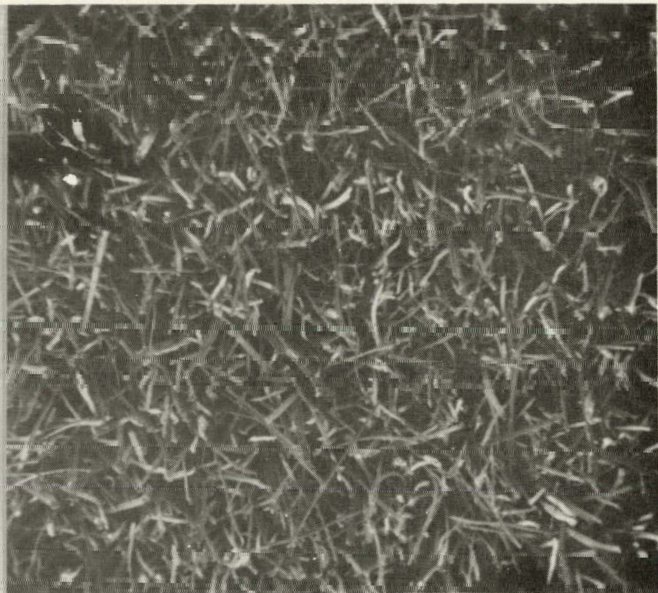


100X

26019-25

FIGURE 21.

FIBER AND 988 C
GRAPHITE (15 w/o) POWDER VIEWED
APPROXIMATELY PERPENDICULAR TO THE
DEPOSIT SURFACE. (ONE OF THE GRAPHITE
PARTICLES IS VISIBLE IN THE CENTER REGION.)



100X

25019-26

FIGURE 22.

FIBER AND
1264 GRAPHITE (5 w/o) POWDER
VIEWED APPROXIMATELY PERPENDICULAR
TO THE DEPOSIT SURFACE.



100X

26019-23

FIGURE 23. FIBER AND 18666-88 GRAPHITE (5 w/o) POWDER VIEWED APPROXIMATELY PERPENDICULAR TO THE DEPOSIT SURFACE.

An attempt to determine the fiber/particulate ratio in deposits was made using a sink-float method. Fibers have a density of about 1.42 gm/cc. Carbon particulates have a density of about 1.90 gm/cc. A 1.68 gm/cc solution of ethylene dibromide in CCl_4 was used as the dispersant. For each composite the ratio of fiber/particulate was significantly greater than that of the starting material. However, it was noted that a clean separation was not possible. Some particles clung to fibers and floated in the solution. The indication, however, is that some particles blow by the deposits without being deposited with fibers.

Rayon Fibers. Rayon fibers were deposited directly on the drum of the bench-model coater using positive 10 kv on the charging wires spaced 1 inch from the grounded drum. Although the rayon fiber deposited readily, the deposits were not as dense as obtained with the graphite fibers. Apparently the charge retained on the deposited fibers prevented the fibers from packing together tightly. Only a few samples about 1/16 inch thick were made with the 10-mil rayon fiber, and no attempt was made to deposit thicker layers because the density of the structure obtained was very low.

Reciprocating Bench-Model Coater

Since the rotating drum was not satisfactory for making thick deposits of fibers, the coater in Figure 24 was constructed to deposit the fibers on a flat surface. The coater consists of the same basic elements as the drum-type unit including (1) a vibratory V-groove feeder and an air venturi to meter the fibers, (2) a duct with a 1/4-inch by 4-3/4-inch slot to distribute the fibers, (3) a reciprocating grounded metal collector plate, and (4) a set of four 0.004-inch diameter charging wires spaced 1-1/2 inches apart and 3/4 inch to 1-1/2 inch above the grounded metal plate. Positive or negative potentials of 8 to 15 kv were applied on the wire to charge and deposit the fibers on the grounded plate as it reciprocated under the wires. The first wire was located approximately 1-1/2 inch from the duct.

As shown in Figure 24, the grounded plate was covered with a Lucite plate with a square or round hole in the area where the fibers were deposited. The sides of the Lucite shaped the fiber deposit, and as the thickness of the deposit increased additional sheets of 1/8-inch or 1/4-inch Lucite were added until deposits up to 1 inch thick were formed.

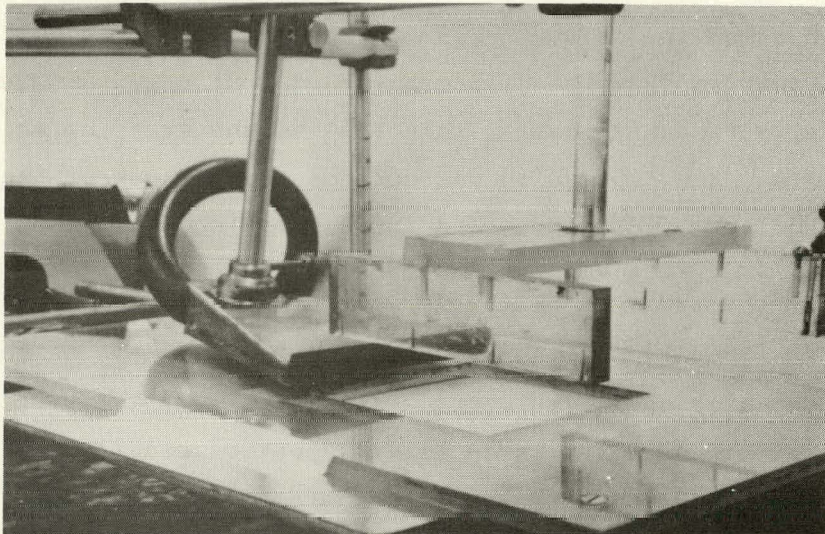


FIGURE 24. RECIPROCATING COATER

Graphite Fibers. Samples of graphite fibers were prepared by depositing the fibers on tympan paper. However, as on the bench-model coater, the deposition rate was extremely low. Although several samples were prepared in the range of 1/16 to 1/2 inch, the thickest samples required at least a day to deposit the fibers. Adjustment of the charging voltage on the wire and the amount of air used to deliver the fiber was extremely critical.

Improved deposition rates were obtained by depositing a solution of about 4 percent coal tar in trichlorethylene with the fibers. The coal tar solution was atomized with a Binks Wren Model A air brush and blown under the first charging wire where it was deposited on the grounded plate. Various techniques were tried including alternating atomization of the coal tar with deposition of the fibers and simultaneous deposition. The latter was the most desirable procedure because it reduced the possibility of producing a layered structure. Deposition of a film of coal tar on a metal plate also made it possible to deposit the fibers without the tympan paper. A sample approximately 1-1/4 inch thick was deposited in less than 2 hours using this technique with continuous spraying of the coal tar solution while the fibers were deposited. Figure 25 illustrates this fiber deposit.

100X

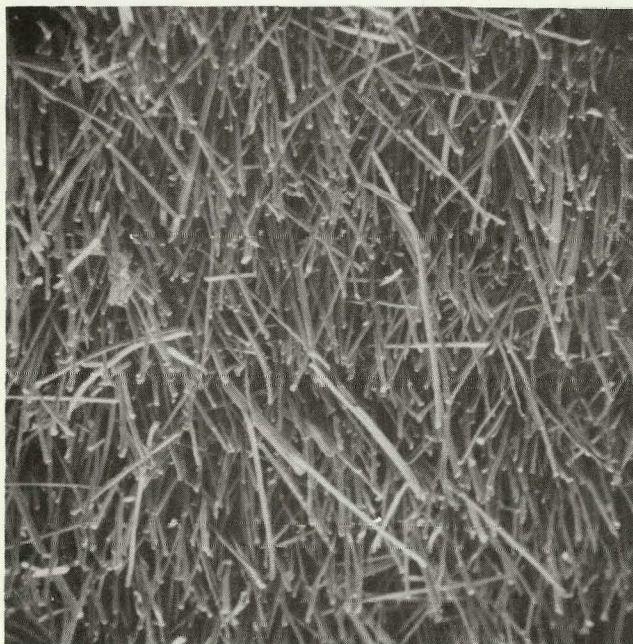


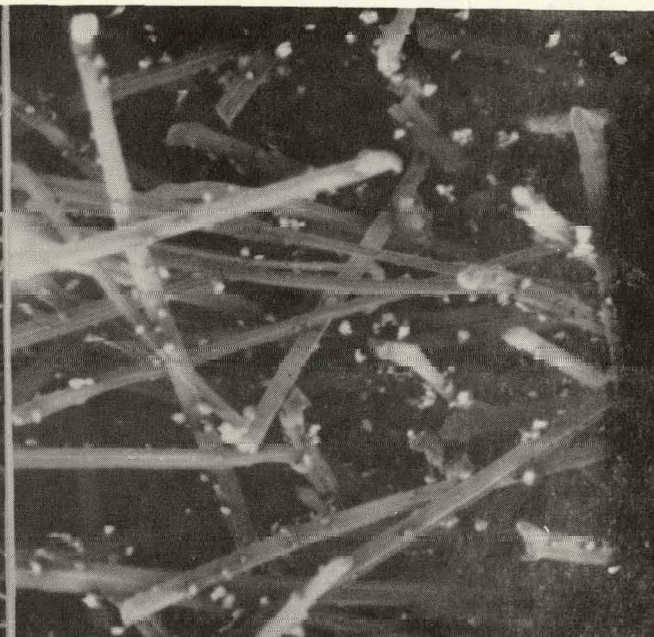
FIGURE 25. ELECTROSTATICALLY DEPOSITED CARBON FIBERS PLUS COAL TAR PITCH AND SOLVENT. VIEW APPROXIMATELY PERPENDICULAR TO THE SURFACE.

Mixing about 10 percent by weight of finely pulverized* coal tar with the fibers also was successful in accelerating the deposition of the fibers. The coal tar was blended with the fibers by passing the coarse-mixed material through a Glen Creston Hammer Mill. The fiber-coal tar mixture was either deposited on tympan paper or on a sheet of aluminum coated with the 10 percent coal tar solution. A 1-inch-thick deposit of the fiber and coal tar mixture was deposited in less than 2 hours with an occasional application of the 4 percent coal tar solution. Figures 26 and 27 illustrate the structure of the fiber deposits and show the pitch particles distributed on the fiber surfaces. Various other thinner samples from 1/6 to 1/4 inch were prepared also.



100X

FIGURE 26.



500X

FIGURE 27.

ELECTROSTATICALLY
DEPOSITED CARBON FIBERS PLUS MICRONIZED
COAL TAR PITCH. VIEW IS APPROXIMATELY
PERPENDICULAR TO THE DEPOSIT SURFACE.

ELECTROSTATICALLY
DEPOSITED CARBON FIBERS PLUS MICRONIZED
COAL TAR PITCH. VIEW IS APPROXIMATELY
PERPENDICULAR TO THE DEPOSIT SURFACE.

* Ground in a 2-inch Micronizer made by the Sturtevant Mill Company, Boston, Massachusetts.

Composites. Only one carbon particle/fiber composite was prepared on the reciprocating plate unit. The composite was made with a mixture of 95 percent graphite fiber and 5 percent Grade 1264 artificial graphite powder classified by sieving to produce particles in the range of 74 to 105 microns**. The mixed composite was deposited on tympan paper to a thickness of 1-1/3 inch in about 4 hours.

Characterization of Deposits. The deposits formed by the reciprocating coater are listed in Table 3 including information on composition, dimensions, density, and fiber orientation. The fiber orientation was qualitatively assessed from scanning electron microscopy of as-deposited samples and by optical microscopy of sections cut through the deposits after impregnation with epoxy. The relevant microphotos (Figures 22, and 25-31) are listed for each in Table 3. The photos show no more than slight deviations from isotropy in any of the samples.

** Powder was sieved through a 150-mesh screen and retained on a 200-mesh screen.

TABLE 3. COMPOSITES PREPARED ON RECIPROCATING COATER

Sample Designation	Composition Fed into Coated, wt. %				Composite (1) Thickness, in.	Composition of Resultant Composite (2)		Approximate (3) Composite Density, gm/cc	ESM Microphoto of Fiber	Preferred Fiber (4) Orientation
	Fiber	Type	Size μ	Amount		wt. % Fiber	wt. % Other			
5 AG/F	95	Artificial Graph	74-105	5	1	96.6	3.4	0.17	Figures 22, 28	Slight tendency to align in plane of deposition.
5 SP/F	100	Pitch/Trichlorethylene	Spray (5)	--	1.2	--	--	0.10	Figures 25, 29	Very slight tendency to align in plane at deposition.
10 MP/F	90	Micronized Pitch	--	10	0.8	--	--	0.08	Figures 26, 27, 30	Isotropic
10 P/F	90	Micronized Pitch	--	10	1.0	--	--	0.08	Figure 31	Preferred alignment in the plane at deposition.

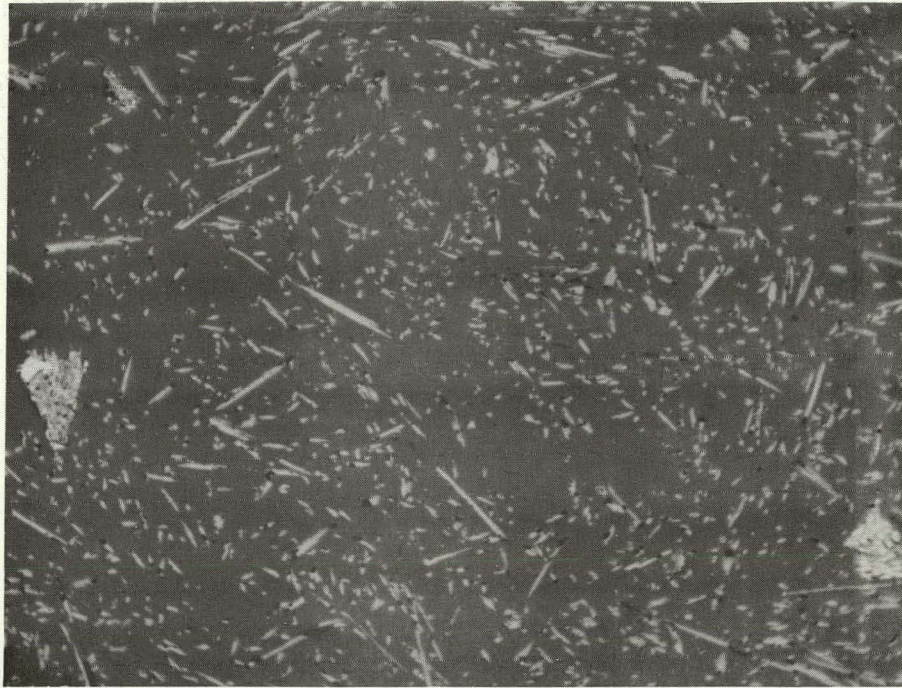
(1) Thickness is average over the 4-inch diameter pad.

(2) Determined by sink/float in liquid having 1.65 gm/cc density.

(3) Average of whole pad and 1-inch square sections taken from pad.

(4) This is a very qualitative judgment of fiber orientation in reference to the plane of deposition and is based on examination of stereo pairs of the ESM photos.

(5) A 4 w/o solution of pitch in trichlorethylene was sprayed on composite as composite was being formed.

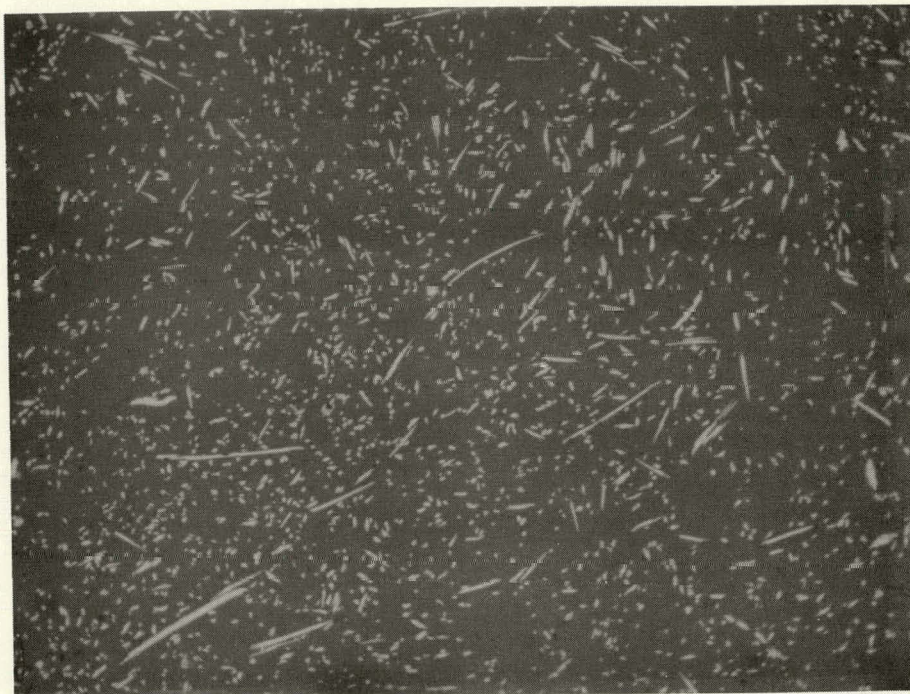


2E525 a. Section Parallel to the Plane of Deposition 100X



2E526 b. Section Perpendicular to the Plane of Deposition 100X

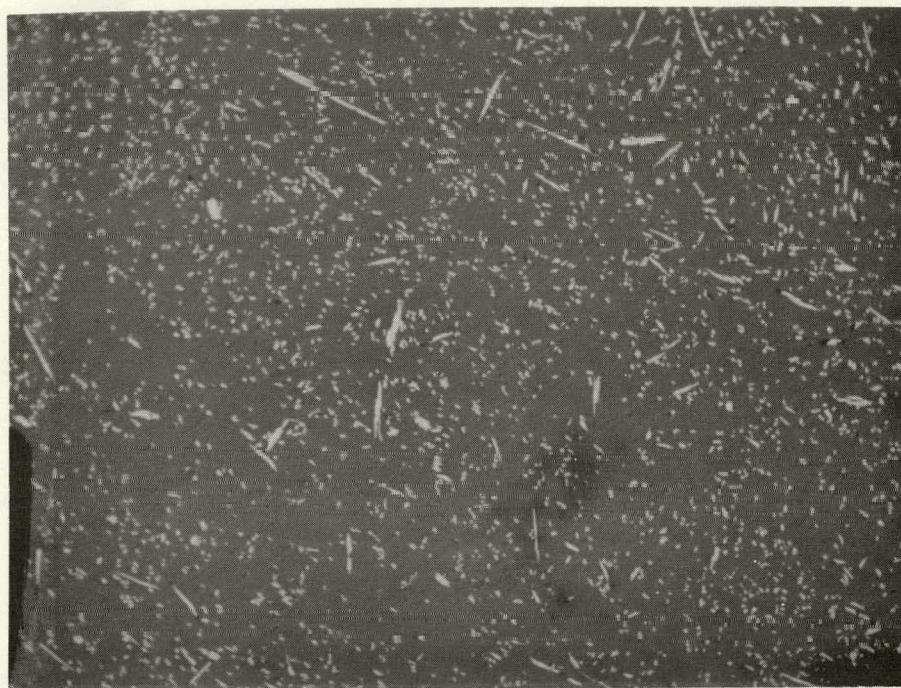
FIGURE 28. POLISHED SECTIONS OF 5AG/F AFTER IMPREGNATION WITH EPOXY.



2E520

100X

a. Section Parallel to the Plane of Deposition

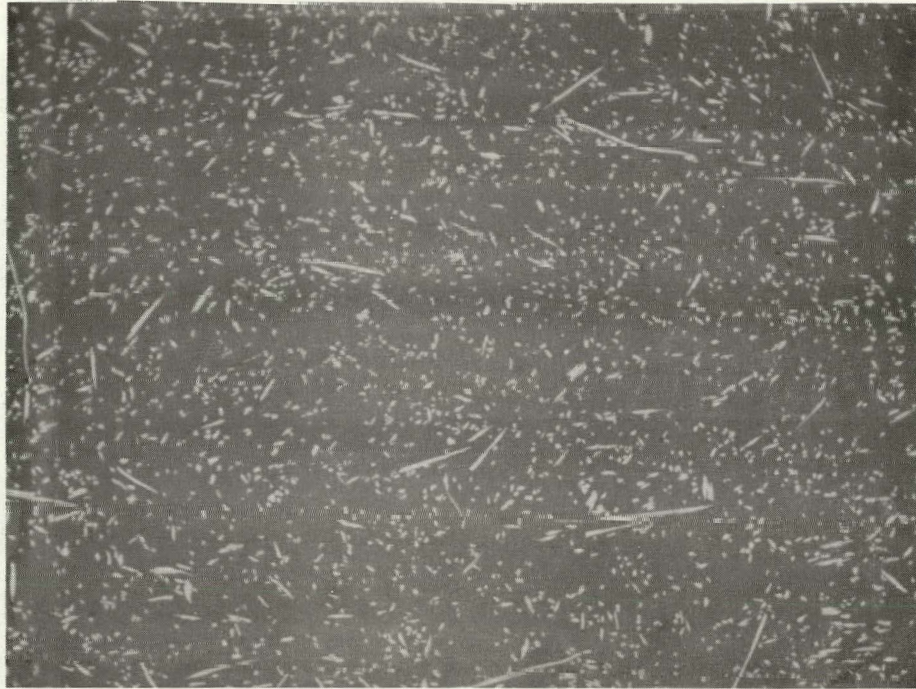


2E529

100X

b. Section Perpendicular to the Plane of Deposition

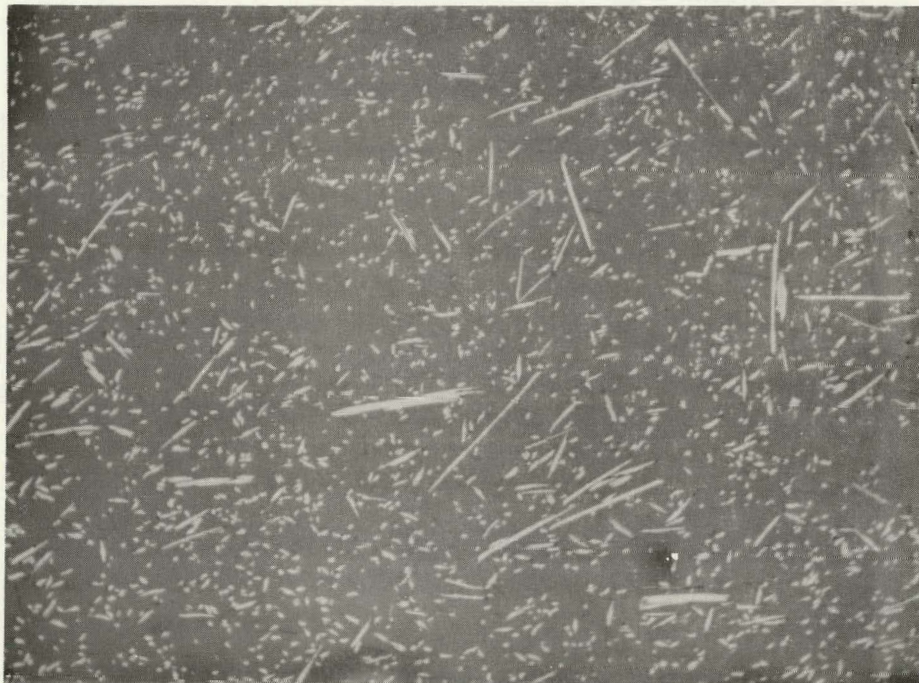
FIGURE 29. POLISHED SECTIONS OF 5SP/F AFTER
IMPREGNATION WITH EPOXY



2E524

100X

a. Section Parallel to the Plane of Deposition

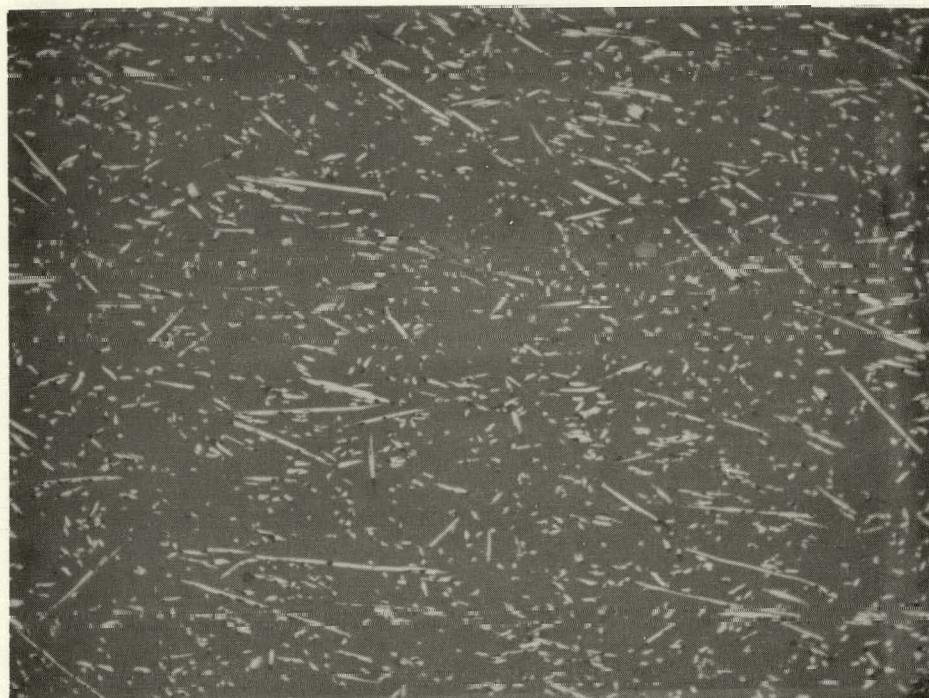


2E523

100X

b. Section Perpendicular to the Plane of Deposition

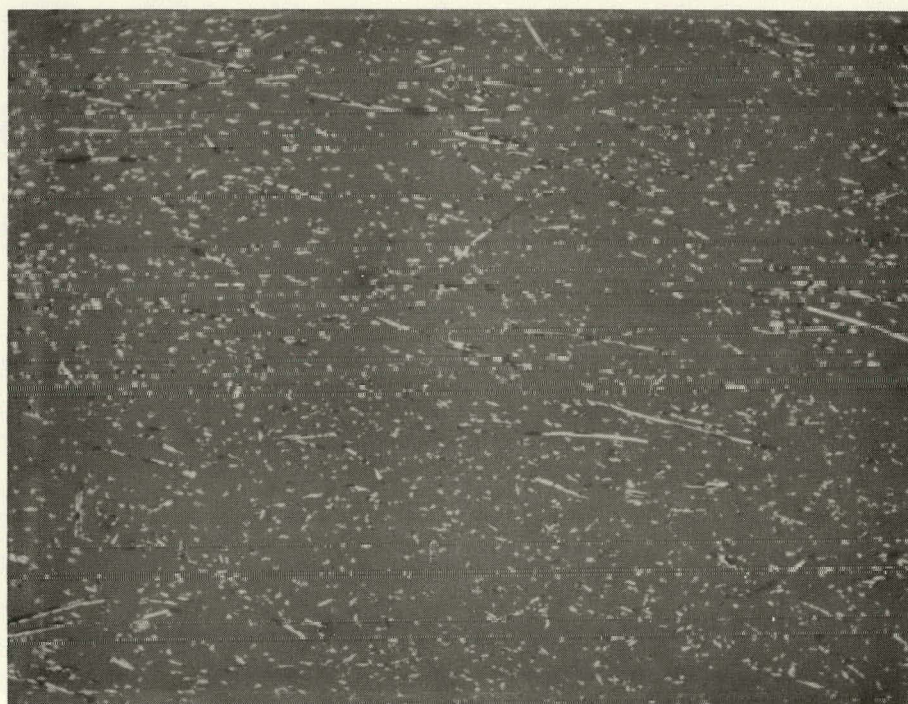
FIGURE 30. POLISHED SECTIONS OF 10 MP/F AFTER IMPREGNATION WITH EPOXY.



2E527

100X

a. Section Parallel to the Plane of Deposition



2E528

100X

b. Section Perpendicular to the Plane of Deposition

FIGURE 31. POLISHED SECTIONS OF 10 P/F AFTER IMPREGNATION WITH EPOXY.

Processing of Deposits

Four pads of composite fiber were available for processing experimentation. The pads were about 4-inches diameter and about 1-inch thick. Processing trials were intended to: (1) stabilize the fiber orientation for orientation studies, (2) determine the preferential ordering imposed on the fibers by uniaxial pressing, and (3) determine the preferential ordering imposed on the fibers by isostatic pressing.

Infiltration

One or two pads of each of the following materials was available for study: (1) 10 percent micronized coal tar pitch in fibers, (2) fibers with continuous spray of 4 percent solution of coal tar pitch in solution with trichloroethylene, and (3) 5 percent 74-105 μ artificial graphite powder with fiber. Each of these materials has a density as deposited of about 0.1 gm/cc. They are very fragile and difficult to manipulate for study. Each pad was cut into approximate 1-inch cubes for infiltration. Infiltration solution included pitch/benzene and starch/water with a small amount of water soluble surfactant.

The materials that contained pitch were difficult to infiltrate with pitch solution. The pitch which formed part of their structure simply dissolved in the solution and, without support, the cubes collapsed. This was especially true for material No. 2 above. However, with firm support on the sides of the cube, and with careful addition of pitch solution, the cubes could be infiltrated.

Starch solution presented no serious problem in collapsing the cubes. However, even with a wetting agent, water does not wet fibers very well. It was therefore necessary to evacuate air from the cube before the starch solution would enter the matrix. The bubbling encountered by this operation could also disrupt the fibers and did except where care was not exercised.

Stabilized, one-inch cubes of these materials were used for further processing and for fiber orientation study as given in other sections of this report.

Uniaxial Pressing

Two materials were uniaxially pressed at pressures of 1 to 2 tons per square inch. A 1-inch cube of material 5AG/F was infiltrated with a solution of 1 gram of No. 30-medium pitch in 7 cc of benzene. The benzene was then removed from the material and the material hot pressed at 1.5 Tsi and 800°C. Apparently, not enough pitch was present to bond fibers together because the material crumbled upon removal from the die. The hot pressed material was not suitable for analysis. Another material (10 MP/F) was infiltrated with a solution of benzene/pitch similar to the 5AG/F material. Three 1-inch cubes of this material were stacked in a mold (about 3 inches high) and uniaxially pressed at 1 Tsi and about 200°C. The material compressed to about 1/2 inch thickness which represents a reduction ratio of about 6:1. The purpose of this operation was to determine the relative amount of ordering which would be imparted to the fibers by uniaxial pressing. The photos of Figures 32 and 33 show the high degree of orientation effected by the uniaxial pressing. Fiber area measurements of a mounted and polished pressed sample (Figure 33) performed using the QTM analyzer show about equal area in sections taken parallel and perpendicular to the pressing direction. The fiber area prior to pressing was also about equal in comparable directions. Moreover, the area of fibers in material after pressing was about 6 x the area in material before pressing, a ratio identical with the volume compaction ratio. These area measurements indicate that no fiber ordering resulted from the uniaxial pressing operation. However, the photomicrographs clearly show that a large proportion of the fibers have turned during pressing such that their axis is perpendicular to the pressing direction.

Isostatic Pressing

One specimen of pitch infiltrated 5AG/F was isostatically pressed at a pressure of 30,000 psi and a temperature of 2,000°F. The purpose of this processing experiment was to determine the isostatic pressing effect on fiber orientation in the material. A 7/8-inch diameter by 1-inch long specimen was bagged in rubber and evacuated. This bagged specimen was then re-bagged in a larger rubber bag with thermax in the space between the bags. The double bagged specimen was then heated overnight in an oven at 200°F and then hydrostatically pressed at 30,000 psi in a water soluble oil solution (room temperature). The

purpose of the thermax was to thermally insulate the material from the relatively cool hydrostatic fluid. As was the case with a similar uniaxially pressed specimen, the material partially fell apart upon removal from the bag. However, enough material remained intact to allow removal of a broken surface for a scanning electron microscope study. Figure 34 is a photograph of the broken surface. The photo shows considerable broken fibers. However, the orientation of the fibers present appears to have remained random. Less pressure would most certainly result in less breakage of fibers. Uniaxial pressing has shown that as little as about 1 Tsi will pack fibers to about half of their theoretical maximum for 3 dimensional ordering. Therefore, suitable isostatic compaction at much lower pressure than 30,000 psi should be possible.

* * * * *

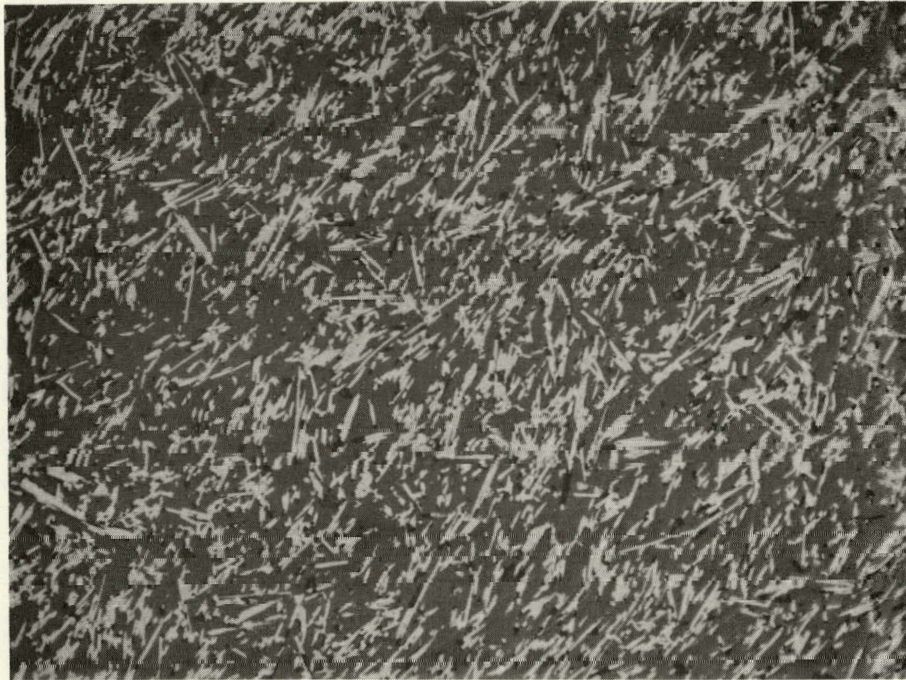
Data for this report are recorded in Battelle Laboratory Record Book 27047, pages 1 through 49 inclusively, and Book 26019, pages 4 through 27.



100X

FIGURE 32. UNIAXIALLY
PRESSED 10 MP/F VIEWED PERPENDICULAR
TO THE DIRECTION OF PRESSURE.

2E532



100X

a. Section Parallel to the Plane of Deposition and Perpendicular to the Direction of Uniaxial Pressure Application.

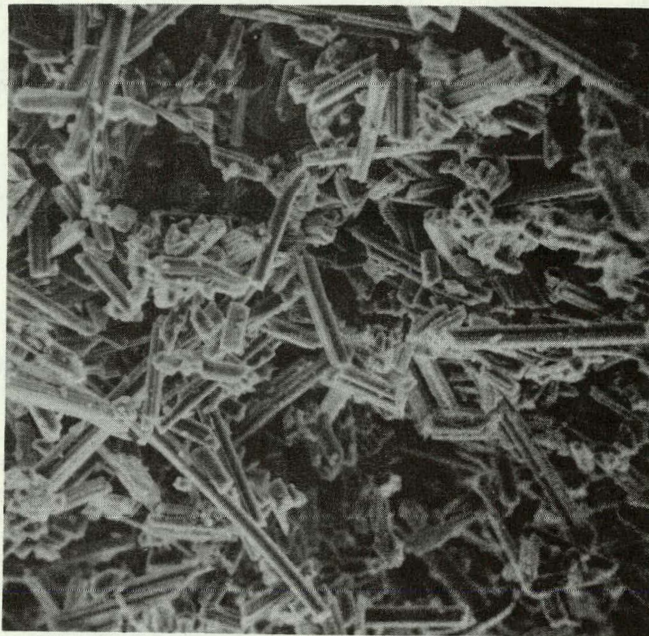
2E531



100X

b. Section Perpendicular to the Plane of Deposition and Parallel to the Direction of Uniaxial Pressure Application.

FIGURE 33. POLISHED SECTIONS OF 10 MP/F UNAXIALLY WARM PRESSED AND BAKED, THEN IMPREGNATED WITH EPOXY.



500X

**FIGURE 34. ISOSTATICALLY
PRESSED 5AG/F.**

DISTRIBUTION:

Division of Space Nuclear Systems
Space Electric Power Office
Washington, D. C. 20545 (3)

Attn: G. P. Dix, Chief,
Safety Branch
H. Jaffe, Chief,
Isotopic Power Systems Branch
C. E. Johnson, Chief,
Reactor Power Systems Branch

USAEC

Division of Technical Information
Hdqs Library G-017
Reports Section
Washington, D. C. 20545

Hdq. Air Force Systems Command (SCIZN)
Washington, D. C. 20331
Attn: Nuclear Safety Branch

Aeronautical Systems Division
Wright-Patterson AFB, Ohio 45433
Attn: Augustus Daniels, SEPRR

Air Force Materials Lab.
Wright-Patterson AFB, Ohio 45433
Attn: M. L. Minges
C. Pratt

Director, AFWL (WLIL)
Kirtland AFB, New Mexico 87117
Attn: Lt. Col. M. N. Nold (WLRB)

Director, AFWL
Kirtland AFB, New Mexico 87117
Attn: Lt. Col. H. L. Harris (WLAS)

Director, AFWL
Kirtland, AFB, New Mexico 87117
Attn: WLIL (E. Lou Bowman)
For: Aerodynamics

Space Systems Division
Air Force Unit Post Office
Los Angeles, California 90045
Attn: Technical Library

Director, USAF Project RAND
Vis: Air Force Liaison Office
The RAND Corp.
1700 Main Street
Santa Monica, California 90406

U. S. Air Force Academy
Aerodynamics Department
Colorado Springs, Colorado 80912
Attn: Prof. Ralph Marker

AF Office of Scientific Research, RDTRRF
Washington, D. C. 20330

Arnold Engineering Develop. Center AFSC
United States Air Force
Arnold AFB, Tennessee 37389

AF Research Division, ARDC
Aeronautical Research Lab.
Wright-Patterson AFB, Ohio 45433

Army Missile Command ARDAB
Redstone Arsenal
Huntsville, Alabama 35806

Ballistic Research Lab.
U.S. Army
Aberdeen Proving Ground
Maryland 21005

Department of the Navy
Gas Dynamics Division
Aerodynamics Lab.
Washington, D. C. 20007
Attn: Dr. S. De Los Samios

Commander
Naval Weapons Center
China Lake, California 93555
Attn: Technical Library

U. S. Naval Ord. Lab.
Aerophysics Division
White Oak, Silver Springs,
Maryland 20900 (2)
Attn: Dr. R. K. Lobb
L. F. Gowen

U. S. Naval Weapons Lab.
Technical Library
Dahlgren, Virginia 22448

Office of Naval Research
Technical Library
Department of the Navy
Washington, D. C. 20390

Naval Postgraduate School
Technical Library
Monterey, California 93940

U. S. Naval Academy
Library
Annapolis, Maryland 21402
Attn: Dr. R. B. Mathieu

Administrator, NASA
Washington, D. C. 20545
Attn: Thomas B. Kerr

NASA, Ames Research Center
Moffett Field, California 94035
Attn: Howard K. Larson

NASA
Goddard Space Flight Center
Glenn Dale Road
Greenbelt, Maryland 20771 (2)
Attn: Charles Baxter, Bldg 21, Rm G-74
Code: 450, A. W. Fihelly,
NIMBUS Project

NASA, Langley Research Center
Langley Station
Hampton, Virginia 23365
Attn: Librarian

NASA, Lewis Research Center (2)
21000 Brookpark Road, Cleveland, O 44135
Attn: George Mandel and L. Nichols

DISTRIBUTION: (Continued)

NASA, Manned Spacecraft Center
Houston, Texas 77058

Attn: Chief, Tech. Info. Division
G. Strouhal, Structures and
Mechanics Division

NASA, George C. Marshall Space
Flight Center
Huntsville, Alabama 35812

Attn: W. Y. Jordan

NASA, Scientific and Tech Info Facility
P.O. Box 33

College Park, Maryland 20740

Attn: NASA Representative, S-AK/DL

Flight Research Center, NASA

P.O. Box 273

Edwards, California 93523

George C. Marshall Space Flight Center,
NASA

Huntsville, Alabama

Attn: Mr. A. R. Felix, R-AERO-AE

DASA, Technical Library

P.O. Box 2610

Washington, D. C. 20301

White Sands Proving Ground

Technical Library

Las Cruces, New Mexico 88002

Advisory Group for Aeronautical

Research and Development

NATA, APO 230

New York City, New York

AC Electronic Defense Research Laboratories

General Motors Corp.

Santa Barbara, California

Attn: Dr. K. S. Wen

Aerojet-General Corp.

Sacramento Plant, P.O. Box 1947

Sacramento, California 95809

Aerospace Corp.

P.O. Box 95085, Los Angeles, Calif. 90045

Attn: W. E. Welsh, Jr.

Aerospace Corp.

2350 E. El Segundo Blvd.

El Segundo, California 90245

Attn: Dr. Harold Mirels

Aerotherm Corp.

485 Clyde Ave.

Mountain View, California 94040

Attn: R. Rindal

AIAA Journal

Technical Literature Digest

500 Fifth Ave.

New York, New York

ARO, Inc., Von Karman Gas Dynamics,

Facility Arnold Air Force Station,

Tennessee 37389

Attn: Jack Whitfield, Mgr., VKGDF

Battelle Memorial Institute (2)

505 King Ave., Columbus, Ohio 43201

Attn: E. L. Foster

F. P. Kirkhart

Bell Aerosystems Co.

P.O. Box 1

Buffalo, New York 14240

The Boeing Co. (3)

P.O. Box 3991

Seattle, Washington 98124

Attn: Maynard D. Pearson

Aerospace Division

W. G. Harris, Flight Tech Lab

Scientific Research Lab

Ford Motor Co., Philco Corp.

Aeroneutronic Div., Ford Road

Newport Beach, California 92660

General Dynamics Corp., Astronautics Div.

5001 Kearny Villa Rd., P.O. Box 1128

San Diego, California 92112

General Electric Co. (2)

Valley Forge Space Tech Center

P.O. Box 8555

Philadelphia, Penn. 19101

Attn: Leon M. Gilbert

E. R. Stover

General Electric Co., Reentry Systems Dept

3193 Chestnut Street

Philadelphia, Penn. 19104

Attn: Mr. John Arnaiz, Mgr.

Aerodynamics Operations

Gulf General Atomic, Inc. (2)

San Diego, California

Attn: G. B. Engle

J. C. Bokros

Gruman Aircraft Eng. Corp.

Bethpage, New York 11714

Hughes Aircraft Co.

Culver City, California 90230

Institute for Defense Analyses

400 Army Navy Drive

Arlington, Virginia 22202

Attn: Richard Briceland

Jet Propulsion Lab

Aerodynamics Facilities Section

Pasadena, California

Attn: Mr. E. A. Laumann, Mgr.

Kaman Nuclear

Colorado Springs, Colorado

Ling-Temco-Vought, Inc.

Aeronautics Division

Eng. Test and Evaluation

P.O. Box 5907

Dallas, Texas 75222

Attn: R. C. McWherter, Mgr.

DISTRIBUTION: (Continued)

Lockheed Missiles and Space Co. (3)
P. O. Box 141
Sunnyvale, California

Attn: H. H. Greenfield, Mgr.
Nuclear Power Devel.
Harold F. Plank
R. C. Lee

Los Alamos Scientific Lab (3)
P. O. Box 1663

Los Alamos, New Mexico 87544
Attn: Report Librarian
L. D. P. King
Morton Smith

The Marquardt Corp.
16555 Saticoy Street
Van Nuys, California 91409
Attn: G. S. Bahn

Martin-Marietta Corp.
Baltimore Division
Baltimore, Maryland 21203

Martin Marietta Corp.
P. O. Box 179
Denver, Colorado 80201
Attn: Dr. T. E. Bowman

Martin Marietta Corp.
Orlando, Florida
Attn: J. Potts

McDonnell Douglas Corp. (2)
Missile and Space System Div.
3000 Ocean Park Blvd.
Santa Monica, California 98406
Attn: Ken Kratsch
R. A. Meyer

McDonnell Douglas Corp.
P. O. Box 516
St. Louis, Missouri 63186
Attn: Dr. A. Lombard

North American Rockwell Corp.
Space and Info. Systems Div.
Meteor Physics
12214 Lakewood Blvd.
Downey, California 90241
Attn: Mr. C. N. Scully

Northrop Corp., Northrop Norair
3901 West Broadway
Hawthorne, California 90250
Attn: Mr. S. A. Powers

Southwest Research Institute
Dept. of Mech. Sciences
8500 Culebra Road
San Antonio, Texas 78228
Attn: Dr. H. N. Abramson,
Director

Southern Research Institute
2000 9th Ave. S.
Birmingham, Alabama 35205
Attn: C. D. Pears

TRW Systems, P. O. Box 287
Redondo Beach, California
Attn: Donald Jortner

Union Carbide Corp., Carbon Products Div.
12900 Snow Rd, Parma, Ohio 44101

Union Carbide Corp., Y-12 Plant
P. O. Box Y, Oak Ridge, Tennessee 27830
Attn: George Marrow

Union Carbide Corp., ORNL
Oak Ridge, Tennessee 37830

Westinghouse Electric Co., Astronuclear Lab
P. O. Box 10864, Pittsburgh, Penn. 15236
Attn: H. P. Smith

Cornell Aeronautical Lab
4455 Genesee St., P. O. Box 235
Buffalo, New York 14225

Illinois Institute of Technology
Chicago, Illinois 60616
Attn: Dr. H. Obremski

AVCO Corp., Missile Systems Div.
201 Lowell St., Wilmington, Mass. 01887
Attn: Dr. A. J. Pallone

AVCO Corp., Space Systems Div.
201 Lowell St., Wilmington, Mass 01187
Attn: Dr. R. R. John, Director

Pennsylvania State University
College of Engineering
University Park, Penn. 16801
Attn: Dr. P. L. Walker
Department of Fuel Science

D. B. Shuster, 1200
R. L. Peurifoy, Jr., 1220
H. W. Schmitt, 1225
T. B. Lane, 1540
D. F. McVey, 1543
T. M. Burford, 1700
A. A. Lieber, 1910
A. W. Snyder, 5220
J. E. McDonald, 5300
H. M. Stoller, 5310
R. C. Heckman, 5322
D. W. Ballard, 7361
R. J. Tockey, 8176
J. C. King, 8300
J. A. Mogford, 8341
A. R. Willis, 8351
G. A. Fowler, 9000
A. Y. Pope, 9300
R. C. Maydew, 9320
B. E. Bader, 9328
I. Auerbach, 9328
K. J. Touryan, 9340
J. K. Cole, 9341
F. G. Blottner, 9343
A. J. Clark, 9510
S. McAlees, 9513
G. C. McDonald, 3416 (4)
W. K. Cox, 3422-1 (15)